University of Zurich[UZH]

Department of Geography

Reconstruction of local vegetation and environmental conditions of a peatland in the Thuringian Forest – assessed by lipid analysis.

GEO 511 - Master Thesis

Author: Silvana Bernasconi

Matriculation number: 11-712-270

Supervised by: PD Dr. Guido Wiesenberg

Co-supervised by: Dr. Klaus-Holger Knorr

Faculty representative: PD Dr. Guido Wiesenberg

June 30th 2017

Department of Geography, University of Zurich

Abstract

Peatlands provide many insights into biogeochemical processes and environmental changes during Holocene. Due to their anaerobic environments, amongst others, compounds of lipids or pollutants like polycyclic aromatic hydrocarbons are preserved. Peatlands grow through accumulating remains of water-loving plants and their height is defined as balance between precipitation, evaporation and outflow. Climate related variations in the peat appear in lipid distributions and enable a reconstruction of vegetation and natural and anthropogenic influences on the evolution of the peat bog. A peatland called Beerbergmoor, located in the Thuringian Forest Biosphere Reserve, serves as an example for reconstruction of Holocene climate change linked to predominant vegetation changes.

Lipid compounds such as *n*-alkanes, *n*-fatty acids and *n*-alcohols were measured by gas chromatography. Distributions of the compounds within the samples give information about past climatic changes. Moreover, relative abundances of polycyclic aromatic hydrocarbons were measured, in order to estimate past anthropogenic impacts on the Beerberg peat.

In times of Bronze age, which corresponds to the oldest (lowest) layers of the Beerberg peat, a shift from cold and wet to warm and dry climatic conditions is indicated by $\delta^{13}C$ composions as well as CPI and ACL values. The predominant vegetation changed from other peat forming plants (e.g. *Calluna vulgaris, Isoleptis setacea*) to *Sphagnum* species. This era is followed by increased precipitation and thus wetter conditions, which favoured growth of *Sphagnum* sp. In the course of time, the dry and warm climate changed to moist and cold conditions. During Migration Period and Early Middle Ages, a shift to even colder conditions were detected. As a result, human activity was reduced during this time, what led to a time with low PAH concentrations. In the Modern Era, which started approximately in the 16th century, a considerable increase of PAHs as well as a shift to warmer climatic conditions was found, what can be traced back to the time of industrialization.

To sum up, major and minor changes of precipitation, humidity and temperature led to short- and long-term variations of climate in the last 4500 years. Shifts in predominant vegetation as well as anthropogenic influences on the peat have been detected.

Content

Figures

Tables

Abbreviations

Abbreviation	Meaning
ACL	Average chain length
AD	Anno domini (after Christ)
A-fraction	Aliphatic hydrocarbons
BC	Before Christ
B-fraction	Aromatic fraction
BSA	N,O-Bis(trimethylsilyl)acetamide
C	Carbon
CAR	Carboxylic acid ratio
C-fraction	Heterocompounds
CPI	Carbon preference index
DCM	Dichloromethane
EPA	US Environmental Protection Agency
FA	Fatty acid
FID	Flame ionization detector
GC	Gas chromatography
H-fraction	Carboxylic acids
HMW	High-molecular weight
KOH	Potassium Hydroxide
LMW	Low-molecular weight
m/z	Mass divided by charge number
MSD	Mass selective detector
N	Nitrogen
N-fraction	Neutral components
PAH	Polycyclic Aromatic Hydrocarbon
P_{aq}	Proportion of aquatic to terrestrial vascular plants
P-fraction	High-molecular weight compounds
pH	Potential of hydrogen
RSU	Ratio of saturated versus unsaturated fatty acids
SIM	Selected ion monitoring
SPE	Solid Phase Extraction
TC	Total carbon
TLE	Total lipid extract
TN	Total nitrogen

1. Introduction

Peatlands cover about 4 x 10^6 km^2 of the earth surface. Some of them are separated in small patches and others are widespread, especially in cooler climate areas such as Canada or Northern Europe (Chambers and Charman, 2004; Clymo, 1998). They provide many insights into biogeochemical processes and environmental change during the Holocene. Thanks to their land location they are more easily accessed than ice sheets or oceans, they do not require the expensive equipment necessary to core lakes, ice or ocean bottoms and they preserve a huge range of proxies for climate, due to the good preservation of organic matter in their anaerobic environments (Chambers and Charman, 2004).

In general, peatlands have a great potential for investigations of local or regional vegetation history (Chambers and Charman, 2004). In particular due to the fact, that vegetation usually reflects local climatic conditions (Pancost et al., 2002; Chambers and Charman, 2004; Belyea and Malmer, 2004). Peatlands normally have a naturally accumulated layer of organic material at the surface produced by various plants such as *Sphagnum* species, which occur in most of them. Some of these *Sphagnum* sp. are important fixers of carbon and especially resistant to other vegetation or extreme climatic events (Clymo, 1998). Certain *Sphagnum* sp. can grow in nutrient-poor conditions and are able to acidify their environment, whereas others prefer nutrient-rich conditions. This is why *Sphagnum* sp. are mostly dominant in peatlands, as they survive changing or extreme conditions (Clymo, 1998). Due to the long lifespan of *Sphagnum* sp. and their response to changing environmental conditions, they are suitable to trace environmental changes, for example through an analysis of lipid patterns and stable isotopes (Wiesenberg and Gocke, 2015).

Peat-forming plants such as Sphagnum contain lipid-biomarkers. For example free or bound lipids like *n*-alkanes or *n*-alcohols are part of soils and peat (Huang et al., 2011). Initially, these biomarkers have been studied in marine settings as proxies for organic matter inputs. Although peatland biomarker studies have not been as extensive and common as ice cores, tree rings or lake sediment studies (Chambers and Charman, 2004), a number of studies of terrestrial settings have already been performed in peatlands (Pancost et al., 2002). Wagner (2013) for example studied two peat bogs in

the Thuringian Forest. The aim of the work was to investigate the relationship between peat decomposition processes and the distribution of elements on a depth profile. Moreover, the output of dissolved organic carbon as well as nutrients and trace elements according to climatic preconditions and precipitation were studied (Wagner, 2013). Nevertheless, not many conclusions were made about the climatic and environmental changes during the evolution of the peat bog. This study therefore focuses on the palaeoenvironmental development of a peatland located in the Thuringian Forest, which was investigated through lipid analysis and stable isotopes. The aim of the study was to detect patterns in lipid distributions and additionally in C and N concentrations. The study was based on the following comprehensive research question: To which environmental conditions has the peatland in the Thuringian forest been exposed in the last 4500 years?

1.1 Scientific background

Blytt (1876) and Sernander (1908) were pioneers of the first systematic Holocene climastratigraphy in Scandinavia (Chambers and Charman, 2004). Blytt (1876) studied different ecosystems and their plants. Amongst others, he investigated different peatlands and determined plants, trees and mosses species that presently occured in the various peatlands (Blytt, 1876). In the end, he was able to describe changes in vegetation assemblages in peat mosses, which had been affected by climatic changes (Sernander, 1908). Although based on these data this author could reconstruct postglacial climatic change, the study was confronted with many uncertainties, as is was only based on visual observations. Sernander (1908) developed these findings and presented correlations between archaeological or botanic-geographical and climatic development. He linked the general development of vegetation in peats to different climatic and archaeological periods. The naturalist had the hypothesis, that the present vegetation of mosses forming the peats are correlated with the uppermost peat-bed and additionally he found out, that different layers of mosses must have grown under different climatic stages (Sernander, 1908). This work set the foundation for systematic stratigraphies of mosses and their relation to climate change.

Peatland types

Gore (1983) summarized the English words swamp, bog, fen, moor, muskeg and peatland under the word “mire”. Others reserve the word “mire” for active peatlands

(Chambers and Charman, 2004). However, they all have something in common: They are built from plants. Thus, aboveground biomass must be considered.
It is known that a great range of different peatland types exists. This starts with Minerotrophic Swamps (rich swamps), which for example have a strong flow of mineral-rich, nearly neutral, water out of the peatland and a water level above the peat surface (Heinselman, 1970). In contrary, Strangmoors, that are distinct drainage channels with high water tables, are slightly to moderately acidic and receive water from mineral soils, precipitation and limited runoff from ombrotrophic peat bogs. Another type of bog is the semi-ombrotrophic or semi-raised bog. Water inflow is possible from one or two sides, whereas water outflow is possible towards two or three sides, what causes a reduction of mineral input. This effect is enhanced through receiving little mineral-soils due to the local relief and thus waters are very acidic (Heinselman, 1970). Even more acidic is the peatland type of the ombrotrophic type or raised bog. Usually, water flow is blocked in both directions due to the convex surface and water tables stand near the surface and are highly acidic (Heinselman, 1970). Ombrotrophic bogs receive water and minerals only from precipitation (ombrotrophic = rain-fed). This normally causes low pHs, few mineral salts and deficiencies in some elements for plants (Heinselman, 1970). Most of the bog profile is constantly underwater and thus many biogeochemical processes slowed down or fully hindered and as a consequence of the reducing conditions organic matter well preserved. This is why ombrotrophic peatlands are suitable for reconstructing environmental change through time.

In general, peatlands can only grow in zones where precipitation is higher than evaporation. This is why they mainly exist in humid, temperate-cold climates, corresponding to the region between approximately 50° and 70°N (Beetz, 2008). The area is limited northwards through colder temperatures and southwards due to low precipitation rates. In Central Europe, respectively in Germany, the main zones of continental raised bogs are in the Bavarian Alps and high altitude areas of the low mountain range (Beetz, 2008). The ombrotrophic peatland called Beerbergmoor or Beerberg peat, which was analysed in this thesis, lies in this area (Fig.1).

Peatland development

Peatlands grow through accumulating remains of water-loving plants and their height is defined as balance between precipitation, evapotranspiration and outflow. Climate changes influence this balance, as the precipitation rates, evapotranspiration and temperatures vary (Zheng et al., 2007).

Therefore, water and air temperature both have impacts on the kind and amount of plants growing, which are the main source of organic matter in peat. These two factors influence microbial activity as well in the following way: Moist and warm seasons favour growth and plant development, but warm conditions favour post-depositional microbial reworking and decomposition of peat, particularly if the water level drops sufficiently to increase air exposure of the deposited organic matter. This is the effect of degradation of peatlands when artificially drained (Zheng et al., 2007). Moreover, due to the history of development, ombrotrophic peatlands have a typical shape. They accumulate organic material on the top and with this develop a convex profile. Usually there is only a small amount of soil biota, which favours mineralisation and reduction of dead plant material (Beetz, 2008).

Furthermore, impermeable or low water-permeable layers under the bog soil lead to retained water and favour the development of anaerobic conditions in the pore water: Plant remains become humified and are preserved as peat. In the upper part of peats, aerobic conditions may still be present, depending on the water balance. This means that degradation and decomposition of plant material by aerobic processes may also be present (Beetz, 2008). Additionally, carbon sequestration power declines with time, even if peat decays very slowly anaerobically. The depth of peat increases with time, leading to an increasing total rate of loss, leading to a decreased rate of accumulation (Clymo, 1998).

Due to the low concentrations of nutrients in rainwater, not all types of plants are able to grow in peat. Thus, specific types of plants become dominant with time. The most common plant species in peatlands are Sphagnum mosses (Beetz, 2008). One important fact distinguishes them from higher plants: They can die in the lower part but continue growing in the upper part towards the top. As a consequence, this characteristic enables peatlands to grow up to 4 meters (Beetz, 2008). At the same time, this is one reason why *Sphagnum* sp. are dominant peat-forming plants in many peatlands (Zhang et al., 2017).

In the oxygen depleted water, *Sphagnum* sp. and other plant remains are better preserved than under aerobic conditions. Thus, bogs can serve as palaeoenvironmental archives and can be used to understand current biogeochemical cycling and to reconstruct plant changes.

As mentioned in a previous section of chapter 1.1, peatlands are used for multiproxy studies of environmental and climatic changes over Holocene and help to reconstruct vegetation history. This is due to the sensitivity to variations in climate and the reaction to changes in precipitation (Chambers and Charman, 2004; Pancost et al., 2002). Additionally, Schellekens and Buurman (2011) mention that a correlation between past vegetation composition and hydrology exist and that peatlands usually have well-preserved stratigraphies.

Peats and climate

Ombrotrophic bogs receive water and nutrients only from the atmosphere and are not influenced by the catchment. Therefore, for example, they can be used to reconstruct temporal changes in local climatic conditions or precipitation-evaporation balance. Peat bogs, in addition, can also be used for example as archives for pollution. Besides water and carbon dioxide, organic pollutants in gaseous phase enter or leave vegetation through the stomata or waxy cuticles of the leaves (Thuens et al., 2013; Zhang et al., 2014). As a consequence, plant remains are preserved with the accumulated pollutants to the peat, making the peat, with its high organic matter content, also an archive for reconstructing the concentration and transport of atmospheric polycyclic aromatic hydrocarbons (PAHs) (Thuens et al., 2013).

Research of the potential of peat bogs as archives has started in the 1970s with quantitative macro- and microfossil analysis and the study of peat humification in order to reconstruct climate (Chambers and Charman, 2004). There are many different methods to reconstruct palaeoenvironmental history from peat bogs. One possibility is the use of plant-derived lipids through a core to detect variations in vegetation type through time. In this context, it is crucial to first study the distributions of lipids in modern plants and compare them with the distributions obtained at different depths in the peat profile. This can be done for example for *n*-alkanes, *n*-alcohols and *n*-fatty acids (Huang et al., 2011), which are common components of plants. These biomarkers can all be used as molecular proxies for reconstructing palaeoenvironmental changes in ombrotrophic peatlands (Schellekens and Buurman, 2011).

n-Alkanes

n-alkanes are primarily produced in the leaves of plants and not in the roots, and they are more or less immobile and deposited sequentially on the peat (Nichols et al., 2006). Generally, C_{23} alkanes and sometimes C_{25} alkanes are quite uncommon in terrestrial settings but abundant in many *Sphagnum* sp. Because the C_{23} alkane has low abundances in peatforming plants other than Sphagnum, C_{23} alkane is a diagnostic Sphagnum biomarker (Pancost et al., 2002). Normally C_{33} alkane is absent or abundant in low quantities in *Sphagnum* sp., so it is a biomarker for other peatforming plants, whereas the summed C_{29} and C_{31} alkanes reflect leaf input from different plants (Pancost et al., 2002; Schellekens and Buurman, 2011). In general, input from higher plants is characteristic for a very strong odd-over-even chain length dominance (Jansen et al., 2006).

n-alkanes are not species-specific but their relative abundance can strongly differ among plant species and thus, indicate changes in dominant vegetation type. In addition, C_{23}, C_{29} and C_{31} alkanes can also reflect the degree of decomposition, as their differing susceptibilities to alteration have influence on their relative abundances (Schellekens and Buurman, 2011).

n-fatty acids

C_{16} and C_{18} fatty acids are part of every cell membrane in organisms, whereby unsaturated fatty acids are more abundant than their saturated relatives. Usually monounsatured fatty acids are more susceptible to degradation than saturated acids. However, both types of fatty acids are sensitive to environmental conditions (Zhou et al., 2005). Distributions of specific fatty acids can be consulted for reconstruction of past climate and vegetation. Input from higher plants usually leads to a strong even-over-odd carbon chain length preference, whilst C_{26}, C_{28} and C_{30} are preferred (Jansen et al., 2006).

n-alcohols

Long-chain *n*-alcohols with an even-over-odd carbon chain length preference are characteristic for higher plant input. Jansen et al. (2006) mention, that abundances of shorter chain lengths (<20) are a signal for microbial input. Distributions of *n*-alcohols can support in making statements about changed climatic factors in the past.

Polycyclic aromatic hydrocarbons

Polycyclic aromatic hydrocarbons are produced during incomplete combustion of organic materials like wood, coal, petrol or oil. They are environmental pollutants, which are generated during emissions from anthropogenic activities such as motor vehicles or cigarette smoke (Abdel-Shafy, 2016; Bezabeh et al., 1999). Nevertheless, some PAHs in the environment originate from natural sources like forest fires or volcanic activities. The biggest anthropogenic sources of PAHs are amongst others residential heating, coal gasification, asphalt production, coke and aluminium production, activities in petroleum refineries and motor vehicle exhaust (Thuens et al., 2013; Abdel-Shafy, 2016).

PAHs occur in a gaseous phases and as sorbent to aerosols. Moreover, atmospheric partitioning of PAH compounds between the particulate and the gaseous phases strongly influence their fate and transport in the atmosphere and the way they enter into the human body and in plants. The removal of PAHs from the atmosphere by dry and wet deposition processes are strongly influenced by their gas/particle partitioning. Atmospheric deposition is a major source for PAHs in soil (Abdel-Shafy, 2016). Whereas pyrene or phenanthrene for example, are part of fossil fuels, benzo(a)anthracene or chrysene are mainly combusted from diesel and natural gas (El Nemr et al., 2007). As already stated, ombrotrophic peatlands contain detailed information about atmospheric pollution and thus partly harmful contaminants (Thuens et al., 2013).

1.2 Aim and research goals

Macrofossils, testate amoebae and pollen from peat sequences have helped in the past to reconstruct palaeoenvironmental information. However, due to decomposition of the organic matter, their use has limitations (Zhang et al., 2014; Schellekens and Buurman, 2011). For example, they may not be well preserved in peat sediments, leading to biased reconstructions. Therefore, more reliable and stable indicators need to be developed (Zhang et al., 2014). Molecular markers have been used in the past to reconstruct vegetation (Schellekens and Buurman, 2011). One possible category of durable molecular markers are *n*-alkanes, as their resistance against decomposition is high and they mostly have a low amount of source specificity (Zhang et al., 2014). Ratios of *n*-alkanes have been used so far for reconstructing vegetation changes

(Zhang et al., 2014). However, it is known that there is a lack of studies for compounds other than *n*-alkanes (Jansen and Wiesenberg, 2017).

As already mentioned, more reliable and stable indicators such as molecular proxies are needed in order to reconstruct palaeoenvironmental information. Thus, one goal of this thesis is to test a multi-molecular marker approach using *n*-alkanes, *n*-fatty acids and *n*-alcohols. With these parameters general statements about palaeoclimate changes such as variations in humidity or precipitation should be possible. Moreover, origins of vegetation inputs and changes in local conditions such as the water level or carbon and nitrogen mineralization should be identified. Climate-related variations in the peat will be assessed through the determination of stratigraphic patterns in lipid biomarker distributions. Another goal is a vegetation reconstruction of the last 4500 years, what will be performed with help of lipid distribution patterns and underlined with a Verhib modelling.

Additionally, as PAHs are preserved in peats as well and data are relatively scarce for presence of PAHs in peat (Bojakoswka and Sokolowska, 2003), relative abundances of different PAHs are measured.
Summarizing, the aim of this thesis is to (1) provide a reconstruction of Holocene climate change in the region of Thuringia and its relation to Holocene global palaeoclimate changes with (2) detection of natural and anthropogenic influences on the evolution of this peat bog.

The main research questions linked to hypotheses of this master thesis can be summed up as follows:

- Vegetation reconstruction: Which characteristics in the peat profile of the Beerberg peat indicate changes in the predominant vegetation?
    - Higher plant input such as *Sphagnum* sp. and other plants like shrubs or sedges (*Calluna* sp., *Vaccinium* sp.) have changed in the past.
    - Shifts in vegetation are visible through alternating dominance of different plant species.

- Climate reconstruction: Which patterns in lipid compound distributions indicate changed climatic conditions during evolvement of the peatland?
    - Lipid distribution patterns indicate changed climatic factors such as precipitation, humidity and temperature.
    - Changes from wet and cold to dry and warm climate conditions are visible, and vice versa.
- In which temporal context can the development of the Beerberg peatland be arranged?
    - The development of the peat bog can be set in context with anthropogenic and natural influences.
    - Approximate time periods in history can be estimated and linked to depths of the Beerberg peat.

2. Material and methods

The Beerberg peatland is one of the three peat bogs located in the Vessertal - Thuringian Forest Biosphere Reserve (Fig. 1), which extends over an area of 170 km^2 and is surrounded by the Thuringian forest (Hellmuth, 2006). It has been designated as the first German UNESCO Biosphere Reserve. The highest elevations in the area are the Grosser Beerberg with 982 m a.s.l. and the Schneekopf with 978 m a.s.l. (Fischer, 2008).

Figure 1: Location of the Beerberg peatland in Thuringia (Germany).

Location in Germany (left), location in Thuringia (middle), satellite image (right) ,maps.google.com, accessed on 14.04.17.

The Beerberg peat extends over an area of 41 ha and belongs to the ombrotrophic peat bogs, what means that it is only nourished and irrigated from rainfall events and little surface water runoff (Fischer, 2008; Wagner, 2013). The peatland lies in a zone with a mean annual precipitation of 1300 mm and a mean annual temperature of 4 °C (Wagner, 2013). The Beerberg peat is located in a zone with atlantic influence and temperate cold-moist climate in the snowy low-mountain range (Fischer, 2008). Lange (1967) mentions that Firbas' (1949) oldest determined sample of the peat profile is from 2500 BC in a depth of 280 and 300 cm, what means that the peat is approximately 4500 years old. However, absolute age detection with e.g. radiocarbon dating was not applied in context of this thesis.

2.1 Sampling

42 peat samples of the ombrotrophic Beerberg bog were collected by a Russian peat corer (peat sampler, Eijkelkamp Agrisearch Equipment BV, Giesbeck, Netherlands) down to a depth of 3.40 m. Between 0 and 83 cm, samples were collected every 6 cm

and between 100 and 340 cm every 10 cm. There is no sample between 83 and 100 cm and the depth of 210 – 220 cm is missing as well.
The following aboveground biomass samples were collected: *Calluna vulgaris, Sphagnum magellanicum, Sphagnum capillifolium, Vaccinium uliginosum, Isoleptis setacea, Vaccinium myrtillus, Eriophorum vaginatum* and *Sphagnum rubellum.*

Seeds and belowground biomass were separated. Seeds in samples were removed due to their high content of lipids, which represent a risk of producing non-representative biomarker abundances. The belowground biomass was analysed and treated as separate sample. In total, there were eight belowground biomass samples. Additionally, in the peat sample of 3 – 9 cm a large amount of grass was found, what was treated as a separate sample as well.

The total of 59 samples were freeze dried and steel ball-milled for minimum 1 minute and with a frequency of 30 with a Retsch MM 400 horizontal mill. In cases where woody stems or fibres of plants still were not sufficiently fine, they were milled one or two minutes longer until being homogenous.

2.2 Elemental analysis

As a next step, the samples were weighted with a Mettler Toledo XS2015 Dual Range. 0.7 to 1 mg of every sample was filled in a tin capsule. Every ten samples, there was a blank tin capsule. The tin capsules were measured on a Thermo Fisher Scientific Elemental Analyser coupled to a Delta V isotope mass spectrometer and the following values were measured in duplicate: Total carbon in mg g^{-1} sample, total nitrogen in mg g^{-1} sample, $\delta\,^{13}C$ and $\delta\,^{15}N$. Carbon and nitrogen isotopes are reported in the conventional delta notation in permil (‰) relative to the VPDB and AIR standard, respectively.

2.3 Lipid extraction and separation

Total lipid extract

Total lipids were extracted with the Soxhlet extraction method. This is a standard technique in geochemistry and food chemistry (Wiesenberg and Gocke, 2015). As only

small amounts of material were available, aliquots between 2 and 3 g per sample were used.

Total lipid extracts were extracted in a Soxhlet apparatus (Fig. 2), using dichloromethane (DCM) with methanol (93:7) as a solvent and with a minimum duration of 24 hours.

Figure 2: Material used for Soxhlet extraction and separation of low polarity fractions.

Soxhlet apparatus (left), SPE columns for separation of low polarity fractions (right), photographed by S. Bernasconi.

Neutral components, carboxylic acids and high-molecular weight compounds

For separating fatty acids from other lipid fractions, solid phase extraction (SPE) columns were used (Fig. 2). Firstly, the glass columns were filled with KOH-coated (5%) silica gel and washed with clean DCM. Solvent for the separation of the first fraction (N-fraction, neutral components) was DCM. For the separation of the second fraction (H-fraction, carboxylic acids) a DCM:formic acid mixture (99:1) was used as a solvent. In order to elute the remaining polar and high-molecular weight compounds (P-fraction) methanol was used (Wiesenberg and Gocke, 2015).

As a next step, the neutral fraction (N-fraction) was separated. The method applied is called Solid Phase Extraction (SPE) for the separation of low polarity fractions. Aim of the method is to separate low polar fractions like aliphatic hydrocarbons and aromatic hydrocarbons from more polar compound groups. Firstly, silica gel 100A was activated at 120°C overnight. Large pasteur pipettes were filled with small amounts of glass wool and activated silica gel (Wiesenberg and Gocke, 2015).

Aliphatic hydrocarbons, aromatic compounds and heterocompounds

The first fraction (A-fraction, aliphatic hydrocarbons containing alkanes, alkenes, steranes etc.) was eluted with hexane. In order to separate the B-fraction (aromatic fraction) with polyaromatic compounds like polycyclic aromatic hydrocarbons, hexane:dichloromethane (1:1) was used as a solvent. The third part was eluted with dichloromethane:methanol (93:7) and contains heterocompounds like ketones, alcohols and acids (C-fraction) (Wiesenberg and Gocke, 2015). Usually the N-fraction is roughly partitioned as follows: 10-15% A-fraction, 10% > B-fraction, 60-80% C-fraction.

2.4 Methylation (H-fraction), derivatisation (C-fraction), GC-measurements

Fatty acids

To be amenable to GC analysis, polar fractions need to be derivatised. Numerous methods are available for derivatisation of fatty acids. Methylation and silylation are commonly applied, however, methylated samples are more stable and thus enable a long storage (Wiesenberg and Gocke, 2015). Wiesenberg and Gocke (2015) recommend methylation for fatty acids. H-fractions were firstly solved in DCM. Secondly, 50 µl of $D_{39}C_{20}$ acid was added as standard. To activate the molecules, 500 µl boron trifluoride/methanol (BF_3/MeOH) was added to the sample, before heating for 15 min at 60°C (Wiesenberg and Gocke, 2015). After cooling down, 500 µl of doubly distilled H_20 was added and the sample centrifuged for 1 minute with 2000 rotations per minute. Glass wool was inserted in glass pasteur pipettes and 0.5 – 1 g sodium sulphate added. The sodium sulphate was rinsed with DCM before adding the H-fraction into the pasteur pipette and collecting the lower organic phase in the vial. By adding DCM and centrifuging the organic part several times, a complete elution of fatty acids was possible (Wiesenberg and Gocke, 2015).

Alcohols

A universal approach for derivatization of high diverse lipid compounds is the silylation. The samples of C-fractions were eluted in 100 – 200 µl DCM and 50 µl D37n-Octadecanol with a concentration of 0.1008 mg/ml were added.

Additionally, 50 µl N,O-Bis(trimethylsilyl)acetamide (BSA) was added before placing the vial on the heating block for one hour at 80°C. After cooling down, DCM was added to adjust the targeted solvent volume for measurements.

Gas chromatography and mass spectrometry

Lipid distributions are measured by gas chromatography or gas chromatography-mass spectrometry (GC/MS) (Schellekens and Buurman, 2011; Wiesenberg and Gocke, 2015). For analysis of aliphatic hydrocarbon fractions, 50 µl of D50 n-Tetracosan with a concentration of 0.1016 mg/ml were added to the samples.

The samples of A-, C- and H-fraction were analysed using an Agilent Technologies 7890B GC-FID system. The chromatographic conditions were as follows: Injector and detector temperature set to 320°C, measurements were performed at a concentration of 10 – 20 µg/µl with 1 µl injected at 70°C in splitless mode. Carrier gas was Helium at a constant rate of 1 ml/min. Temperature program was the following: Oven temperature is ramped at 5°C/min until 120°C, 2°C/min until 210°C and 3°C/min until 320°C (Wiesenberg and Gocke, 2015). The B-fraction was measured with selected ion monitoring (SIM method) with an Agilent Technologies 6890N Network GC-MSD system. Specific PAHs (Tab. 1, App.) within mass range m/z 50 – 500 were determined for this thesis and used for quantitative determinations on both gas chromatographs/spectrometers. PAHs are monitored by the US Environmental Protection Agency (EPA) (Lerda, 2011).

2.5 Verhib modelling

The Verhib modelling was performed in Matlab R2017a. Values of *n*-alkanes, *n*-fatty acids and *n*-alcohols per g C were used as input for the script. Moreover, types of aboveground biomass as well as sample depths were needed. The output model contains a modelled overview of peat depths and the corresponding proportions of aboveground biomass. The modelling was performed with both sensitivity parameters set to 0.5.

2.6 Statistics

Mean and standard deviation of N and C values and $\delta^{13}C$ isotope values are integrated in the corresponding figures (Fig. 3, 4 and 7).

3. Results

In the following section, results are presented. They are arranged according to their type (C/N, alkanes, alcohols, fatty acids, PAHs).

3.1 Elemental analysis

Total carbon varies between 410 and 460 mg g^{-1} (Fig. 3) in peat samples. The smallest concentrations lie in depths of 0 – 6 cm and 260 – 265 cm and the highest concentrations at depths of 275 cm, 310 cm and 330 cm. Between a depth of peat surface to 2 meters, the carbon concentrations vary irregularly and peak at 110 cm. Then a section of lower carbon amounts around 420 mg g^{-1} follows until reaching a depth of 265 cm. The carbon content increases afterwards with increasing depth until 275 cm and in deeper layers starts varying again.

Total nitrogen varies between 3.3 and 21.4 mg g^{-1} sample (Fig. 4). The minimum value occurs in a depth of 120 cm and the maximum value at 11 cm. In the first half meter of the profile, most values vary between 5 and 9.8 mg g^{-1}, except some single values. A decrease of nitrogen with increasing depth, which starts at 50 cm, is visible until reaching a depth of 260 cm with values between 3.3 and 5 mg g^{-1}. Afterwards nitrogen values increase again with decreasing depth.

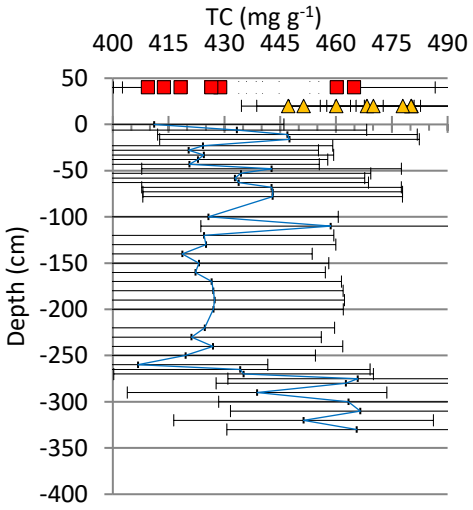

Figure 3: Total carbon concentrations of all samples.

In peat samples (blue line), aboveground biomass samples (red squares), belowground biomass samples (orange triangles). Standard deviations: Peat samples (34.9), aboveground biomass (26.4), belowground biomass (12.6) indicated (black bars).

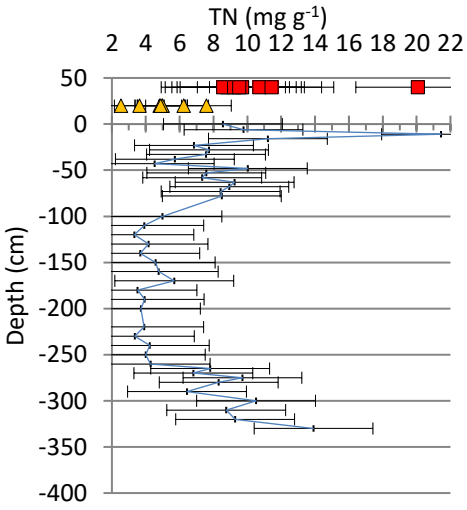

Figure 4: Total nitrogen concentrations of all samples.

In peat samples (blue line), aboveground biomass samples (red squares), belowground biomass samples (orange triangles). Standard deviations: Peat samples (3.51), belowground biomass (1.47), aboveground biomass (3.67) indicated (black bars).

Total carbon in aboveground biomass samples varies between 410 and 480 mg g^{-1}, whereas the three *Sphagnum* sp. have the lowest amounts (Fig. 3). *Calluna vulgaris* and the two *Vaccinium* sp. have the highest concentrations.

Nitrogen varies between 8.6 and 20 mg g^{-1} (Fig. 4). A much higher concentration of N is found in *Isoleptis setacea*, whereas the rest of the aboveground biomass samples all have lower amounts around 10 mg g^{-1}. Compared to peat samples, total carbon concentrations of aboveground biomass samples lie in the same range. However, nitrogen concentrations are slightly lower in peat samples than in aboveground biomass samples.

Belowground biomass samples have total carbon amounts between 450 and 480 mg g^{-1} (Fig. 3). Moreover, they have a nitrogen range of 4.8 to 7.6 mg g^{-1}. The single grass sample has a comparably low concentration of carbon, whereas the nitrogen value is comparably high (Fig. 4). The lowest carbon and nitrogen amounts are found in the belowground biomass sample which corresponds to biomass of depths in 160 to 230 cm.

C and N values can be combined to clusters (Fig. 5). Belowground biomass samples have high C and low N values, whereas most of the peat samples have low N and more or less low C concentrations. Aboveground biomass samples form two clusters, both with low N concentrations but different C concentrations.

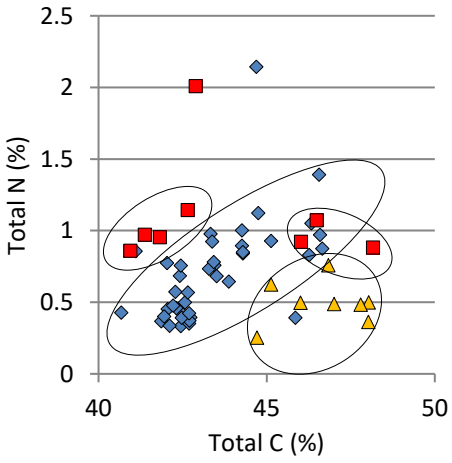

Figure 5: C and N values of all samples.

Peat samples (blue rectangles), belowground biomass (orange triangles), aboveground biomass (red squares). Clusters formed according to the sample type and regarding C and N values, outliners not included.

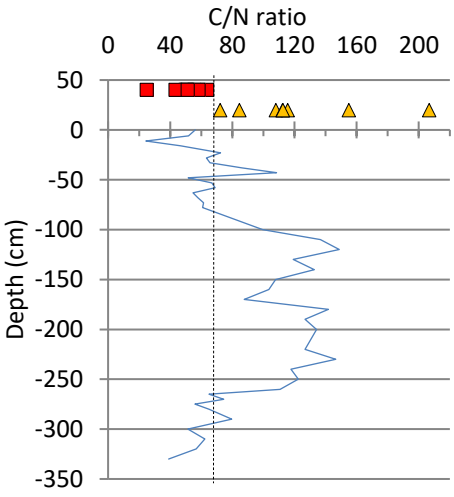

Figure 6: C/N ratios of samples.

Peat samples (blue line), belowground biomass (orange triangles), aboveground biomass (red squares), border between aboveground and belowground biomass samples (dashed line).

Results indicate, that shifts in C/N ratios occur in the peat profile (Fig. 6). In layers below the surface, C/N ratios are comparably low and vary around 70 in the upper 50 cm of the profile with one peak in a depth of 43 cm. These variations are followed by an increase to ratios of 150 until 1.2 m, where the values start to vary again around 130 with increasing depth. Then ratios decrease considerable at about 2.3 m to ratios around 40 with increasing depth.

Belowground samples have C/N ratios between 72 and 206 (Fig. 6), with 206 being the highest value compared to the surface samples, indicating that nitrogen is preferentially reminrealized in the subsurface. Aboveground biomass samples range from 24 to 63, what are low values compared to belowground biomass and peat samples.

$\delta^{13}C$ composition

$\delta^{13}C$ isotope values of aboveground biomass samples range from -25 to -29 ‰, wherby especially *Sphagnum capillifolium, Sphagnum rubellum* and *Calluna vulgaris* have the lowest compositions of $\delta^{13}C$. *Eriophorum vaginatum* has comparably the highest $\delta^{13}C$ isotope value with -25 ‰. In belowground biomass samples all samples have compositions between -24.1 and -28.8 ‰, what can be seen through a small standard deviation (Fig. 7). The lowest isotope value has been found in belowground biomass in depths of peat sample numbers 31 and 39 (Tab. 2, App.).

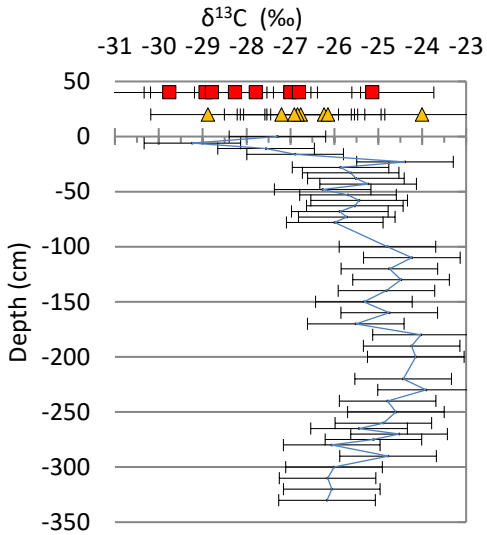

Figure 7: $\delta^{13}C$ compositions of all samples.

Peat samples (blue line), belowground biomass (orange triangles), aboveground biomass (red squares). Standard deviations: Peat samples (1.1), aboveground biomass (1.4), belowground biomass (1.3) indicated (black bars).

δ ^{13}C composions are comparably low in upper layers (Fig. 7). Isotope values start to increase in a depth of 6 cm. The trend of increasing values with increasing depth continues until reaching 1.8 m, followed by a slight decrease until 3.4 m with compositions between -24 and -26.1 ‰.

3.2 Total lipid extract

Total lipid extracts (TLE) in mg lipids per g sample were extracted (Fig. 24, App.). Surprisingly, the TLE of peat sample 38 in a depth of 3 m is more than double compared with the other samples. The figure shows that towards deeper layers of the peat total lipid extracts increase.

Aboveground and belowground samples have total lipid extracts between 20 and 40 mg per g lipid (aboveground biomass) and between 20 and 60 mg per g lipid (belowground biomass). The highest amount of lipids was found in belowground biomass sample 17 – 22 (Tab. 2, App. for depths).

3.3 *n*-alkanes

On average, the most abundant alkane is C_{31}. However, there are some exceptions: Peat sample 30 (230 – 240 cm depth) peaks at C_{25} alkane, peat samples 39 (300 – 310 cm depth) and 42 (330 – 340 cm depth) and belowground biomass sample 54 (Tab. 2, App) have the highest abundance of C_{33} alkane. C_{27} alkane is dominant in *Vaccinium myrtillus* and C_{29} has the highest relative proportion in belowground sample 59 (Tab. 2, App). The typical odd-over-even preference is nevertheless strongly pronounced what means that clearly odd numbered alkanes are highly preferred (Fig. 8). An excerpt of abundances of C_{17} to C_{35} alkanes are shown in the following section. The samples mentioned in the figure refer to a peat depth of 33 to 73 cm.

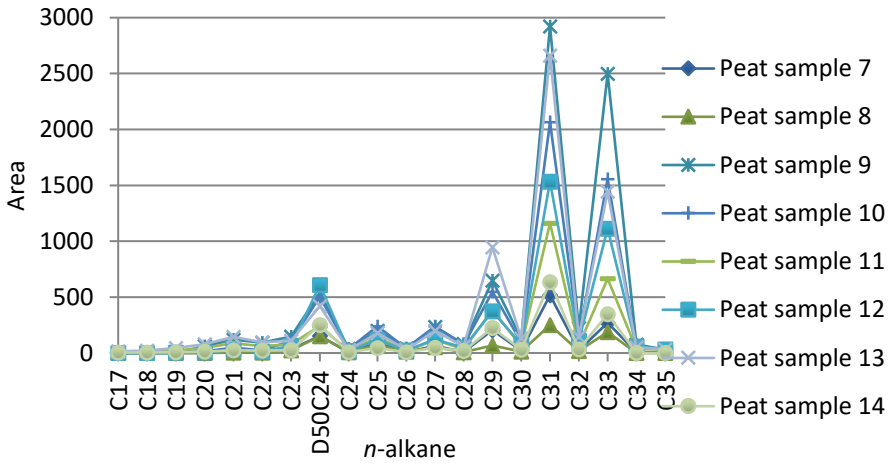

Figure 8: Excerpt of abundances of C_{17} – C_{35} alkanes in samples 7 to 14.

Preference of odd numbered alkanes visible, $D_{50}C_{24}$ standard between C_{23} and C_{24} alkane.

Relative proportions of different *n*-alkanes can be used as indicators for vegetation change, as chain lengths differ from peat forming plant to plant (Zhang et al., 2014). Zhang et al. (2014) mention in their studies, that C_{23} and C_{25} alkanes are indicative for *Sphagnum* sp. and submerged and floating vascular plants. Moreover, long-chain alkanes such as C_{27} and C_{31} are typical for woody and herbaceous plants, whereas C_{29} and C_{31} are characteristic for shrubs (Zhang et al., 2014). These findings were presented in earlier years by Zheng et al. (2007), who additionally mention C_{17} being indicative for aquatic algae and photosynthetic bacteria (Zheng et al., 2007). Generally, it can be said, that high abundances of C_{21}, C_{23} or C_{25} alkanes indicate submerged and floating macrophytes (Zheng et al., 2007; Zhang et al., 2014), whereas C_{27}, C_{29} and C_{31} alkanes refer to vascular land plants and macrophytes (terrestrial plants). In order to test this, abundances of specific *n*-alkanes can be plotted. The results will be discussed in chapter 4.

Whilst C_{23} and C_{25} follow a similar trend, C_{25} and C_{31} are reversed (Fig. 20, App.). Relative proportions of C_{25} and C_{23} alkanes are high near the peat surface and decrease after 6 cm with decreasing depth.

An increase of C_{25} and C_{23} alkane proportions is visible after 50 cm depth, before decreasing again after 1 m. Then a varying phase until a depth of 2.50 m follows, before dropping at a depth of 2.5 m. C_{29} and especially C_{31} alkane have higher relative proportions and are distinctive, primarily where C_{25} and C_{23} alkane have low relative proportions. C_{29} and C_{31} respectively C_{25} and C_{23} follow similar trends, but vice versa.

The ACL (average chain-length) describes the average number of carbon atoms based on the concentrations of long-chain lipid compound homologues. An estimation of fresh higher plant input vs. degraded biomass and microbial remains is possible. In other words, it is described as the weighted mean lipid compound chain length (Zhang et al., 2014; Wang et al., 2016).

$$ACL_{alk} = \sum(z_n * n) / \sum z_n \quad (1)$$

Numerous studies, including Wang et al. (2016), explain the ACL values as a function of temperature, with higher ACL values indicating warmer climates and in reverse. ACL calculations were performed for fractions of *n*-alkanes, *n*-fatty acids and *n*-alcohols. *n* in the formula refers to the number of carbons within a compound and n_z to the quantity of the compound (Wiesenberg and Gocke, 2015).

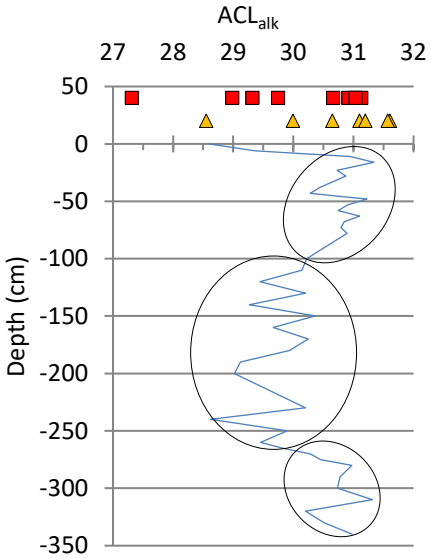

Figure 9: ACL_{alk} of all samples.

Values of C_{25} to C_{35} *n*-alkanes used for calculations. Peat samples (blue line), belowground biomass (orange triangles), aboveground biomass (red squares). Clusters formed regarding ACL_{alk} values <30.5 and >30.5.

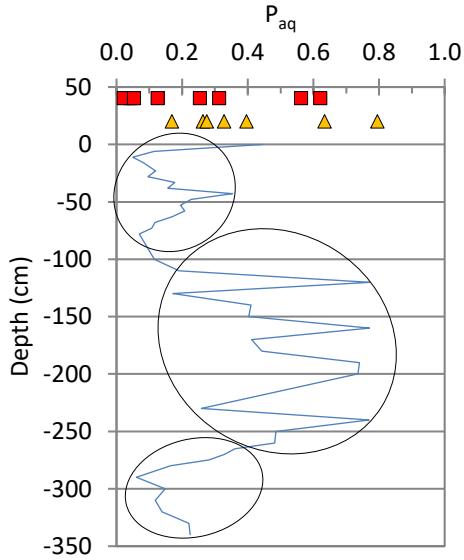

Figure 10: P_{aq} values of all samples.

Peat samples (blue line), belowground biomass (orange triangles), aboveground biomass (red squares). Clusters formed regarding general trend of values and range of P_{aq} values.

The ACL_{alk} values of long-chain *n*-alkanes vary slightly between 28.6 and 31.3 within the peat profile (Fig. 9). Values remain around 31 in the upper meter of the profile. After that, ACL values decrease to 29 - 30 with decreasing depth until reaching 2.50 m. In greater depths below a depth of 2.5 m, values increase again to 30.5 - 31.

A shift from higher to lower values with decreasing depth, followed by an increase with decreasing depth is visible, why shifts in climate may be expected. This will be discussed in chapter 4. Aboveground and belowground biomass samples lie in a similar range as peat samples.

The P_{aq} value describes the proportion of aquatic plants to terrestrial vascular plants, based on the fact that C_{23} and C_{25} are abundant in submerged and floating macrophytes and *Sphagnum* sp., whilst C_{29} and C_{31} occur in terrestrial vascular plants (Zhang et al., 2014). As Wang et al. (2016) propose this proxy to reflect the relative abundance of *Sphagnum* sp. over other bog-forming plants, higher P_{aq} values are expected in *Sphagnum* sp. dominated stages (Zhang et al., 2017). High P_{aq} values (normally > 0.4) are characteristic for fresh *Sphagnum* sp. in peatland settings (Zhang et al., 2017).

$$P_{aq} = (C_{23} + C_{25}) / (C_{23} + C_{25} + C_{29} + C_{31}) \qquad (2)$$

A shift in P_{aq} values is visible (Fig. 10). They keep relatively low between 0.05 and 0.2 until 1.5 m depth, followed by an increase of values with decreasing depth until 2.5 m and values around 0.8. Suprisingly, after 2.5 m the values drop again to values between 0.06 and 0.3 and reach the minimum value of 0.06 in a depth of 3 m. It is possible to form clusters regarding their depth and values.

The CPI (carbon preference index) summarizes the predominance of odd-numbered over even-numbered n-alkanes (Wang et al., 2016). In other words, it describes the distributions of relative proportions regarding even and odd n-alkanes or in general carbon molecules (Zhang et al., 2014; Zheng et al., 2007). Usually values > 1 can be expected, except with belowground biomass, where values < 1 can be awaited and occur (Wiesenberg and Gocke, 2015). Moreover, Wang et al. (2016) mention in their studies that higher plants normally have CPI_{alk} values > 4. If degraded or matured organic matter occurs, low CPI_{alk} values are abundant. This usually results from microbial reworking and cracking, which is damped under cold and dry conditions and leads to higher CPI_{alk} values (Wang et al., 2016).

$$CPI_{alk} = [(\sum C_{21-29\,odd} / \sum C_{20-28\,even}) + (\sum C_{21-29\,odd} / \sum C_{22-30\,even}]/2 \qquad (3)$$

The CPI_{alk} values of peat samples vary between 3.5 and 12.6. They begin to increase from the top towards 38 cm, before dropping down to 3.9 at a depth of 50 cm. Then an increase of values with increasing depth follows, before declining again after the first meter in the profile. At a depth of 2 m values constantly increase again with decreasing depth. In 2.4 m depth, the values start to decrease constantly (Fig. 11). Aboveground biomass samples have varying CPI_{alk} values between 2.2 and 9, whereby belowground biomass samples have rather low values under 6.2, compared to peat samples. Due to low or no abundances of even carbon numbered alkanes, the indexes of two samples could not have been calculated (CPI_{alk} = 0).

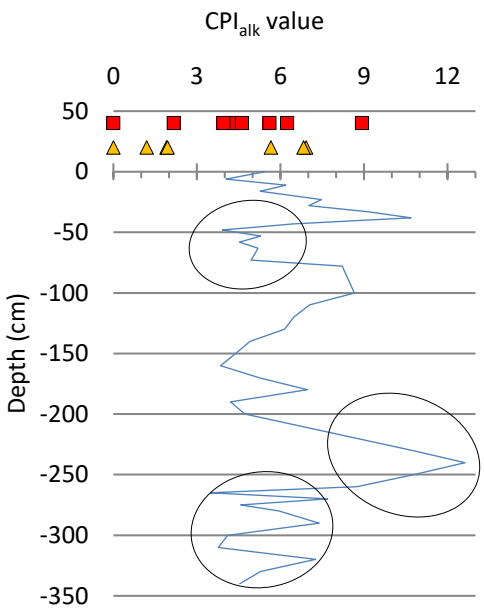

Figure 11: CPI_{alk} values of all samples.

Values of C_{21} to C_{29} alkanes used for calculations. A CPI_{alk} of zero indicates no or very low abundances of even carbon numbered alkanes. Peat samples (blue line), aboveground biomass samples (red squares), belowground biomass samples (orange triangles). Clusters formed regarding accumulation of comparable CPI_{alk} values in similar depths, outliners not included.

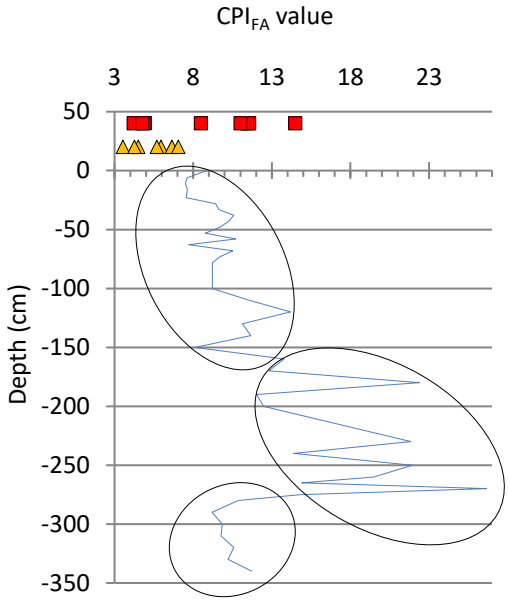

Figure 12: CPI_{FA} values of all samples.

Values of C_{20} to C_{28} fatty acids used for calculations. Peat samples (blue line), aboveground biomass samples (red squares), belowground biomass samples (orange triangles). Clusters formed regarding accumulation of comparable CPI_{FA} values in similar depths, outliners not included.

3.4 *n*-fatty acids

CPI_{FA} values generally have an increasing trend with increasing depth (Fig. 12). They increase throughout the profile until 2.7 meters, followed by a slight decrease afterwards. The values range from 8 to approximately 27. Irregular variations are visible throughout the peat profile. Short interruptions in the increasing trend are visible in depths of 1.2 m, 1.8 m and 2.7 m.

Compared to peat samples, above- and especially belowground biomass samples have lower CPI_{FA} values. They are scattered between 3.5 and 6.6 (belowground biomass) and 4.2 and 14.5 (aboveground biomass samples).

$$CPI_{FA} = [(\sum C_{20-28\,even} / \sum C_{19-27\,odd}) + (\sum C_{20-28\,even} / \sum C_{21-29\,odd})]/2 \qquad (4)$$

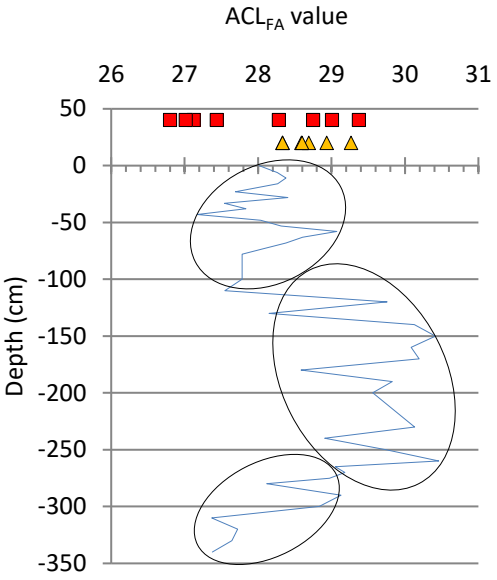

Figure 13: ACL_{FA} values of all samples.

C_{25} – C_{34} fatty acids used for calculations. Peat samples (blue line), aboveground biomass samples (red squares), belowground biomass samples (orange triangles). Clusters formed regarding accumulation of comparable ACL_{FA} values in similar depths, outliners not included.

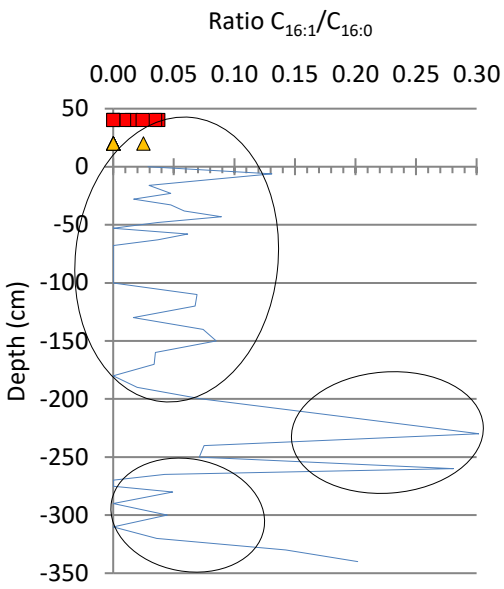

Figure 14: $C_{16:1}/C_{16:0}$ fatty acid ratios of all samples.

Peat samples (blue line), aboveground biomass samples (red squares), belowground biomass samples (orange triangles). Ratios of zero indicate that there were no unsaturated $C_{16:1}$ fatty acids present. Cluster formed regarding accumulation of comparable $C_{16:1}/C_{16:0}$ fatty acid ratios in similar depths, outliners not included.

ACL_{FA} values of peat samples start with low values between 27 and 29 from the peat surface until a depth of 1 m (Fig. 13). With increasing depth, an increase of values up to 30 is visible. A down warded shift in ACL values after 2.5 m follows and values get back to between 27 and 28. ACL_{FA} of aboveground and belowground biomass are scattered within the range of 26.8 and 29.4, whereas belowground biomass samples all have higher values between 28 and 29.3.

Zhou et al. (2005) mention, that the proportion of short-chain unsaturated fatty acids can be expected to be preferentially degraded more due to the fact that microbial alteration is sped up under warm climatic conditions. In order to analyse this fact, ratios

of unsaturated ($C_{16:1}$) and their saturated relatives ($C_{16:0}$) can be calculated (Fig. 14). Values of zero indicate that there were no unsaturated fatty acids in the sample found. All peat samples have values scattered between 0.02 and 0.1, with a few outliners which are higher than 0.1.

$C_{18:1}/C_{18:0}$ ratios show that in top layers ratios are slightly higher than in bottom layers with a decrease of values with increasing depth (Fig. 23, App.).

3.5 *n*-alcohols

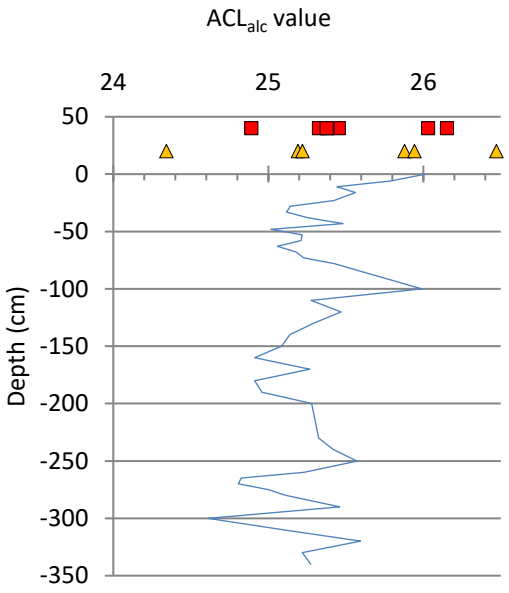

Figure 15: ACL_{alc} values of all samples.

ACL C_{20} – C_{28} alcohols used for calculations. Peat samples (blue line), aboveground biomass samples (red squares), belowground biomass samples (orange triangles).

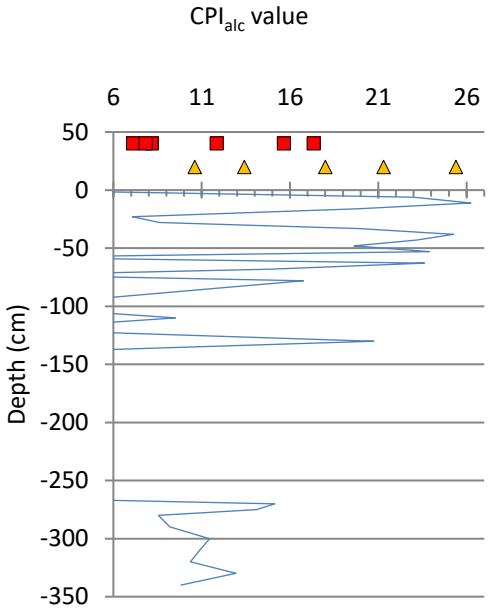

Figure 16: CPI_{alc} values of all samples.

CPI C_{22} - C_{32} alcohols used for calculations. Peat samples (blue line), aboveground biomass samples (red squares), belowground biomass samples (orange triangles).

ACL_{alc} values of *n*-alcohols in peat samples range between 24.1 and 25.5 (Fig. 15). There are no trends visible, as the variations throughout the profile are rather small. Aboveground and belowground biomass samples show similar values, except of two belowground biomass samples, which have lower values. The only visible trend is between 48 and 100 cm with increasing values with increasing depth, followed by a decrease of values with increasing depth.

CPI_{alc} values have such a broad range of values, that it is only possible to make vague statements, such as that the values in deeper layers are lower than in higher layers. Due to missing detected odd numbered n-alcohols, calculations are hindered and results incomplete, especially in a depth between 1.4 m and 2.7 m (Fig. 16).

$$CPI_{alc} = [(\sum C_{22-32\,even} / \sum C_{21-31\,odd}) + (\sum C_{22-32\,even} / \sum C_{23-33\,odd})]/2 \quad (5)$$

For wax lipids generally, *n*-alkanes, *n*-alcohols and *n*-fatty acids with longer chain lengths (>20) and a distinct odd-over-even (*n*-alkanes) or even-over-odd (*n*-alcohols and *n*-fatty acids) chain length predominance is considered to be higher plant derived, whereas shorter chain length homologues are considered to be predominantly of microbial origin (Jansen and Wiesenberg, 2017). This is verified within all three compounds.

3.1 Polycyclic aromatic hydrocarbons

It is known, that PAHs are not degraded over long time, they are immobile once deposited to the peat. Thuens et al. (2013) conclude, that due to methodological restraints, peat cores are inappropriate to display short-time events. In this context, Malawska et al. (2006) questioned, if contaminants are immobile within the profile. They found more low-molecular weight (LWM) PAHs than high molecular weight (HMW) PAHs in deeper layers and came to the result that there should be a down moving of LMW PAHs (Thuens et al., 2013). On the other hand, Thuens et al. (2013) did not observe the same. PAH concentrations show a relatively sharp increase of most masses the upper part of the profile, what is considered to be due to industrialization (Thuens et al., 2013). An increase of PAH concentrations is also visible on results in the Beerberg peat in depths of 11 cm, 28 cm and 53 cm (Fig. 17). A fully quantitative analysis of PAHs was impossible due to missing experience and the difficulty of PAH detection through GC/MS and thus, only relative abundances of PAHs in different depths of the peatland were measured (Fig. 17). Different PAHs were grouped according to the number of aromatic ring systems. The results will be discussed in chapter 4.

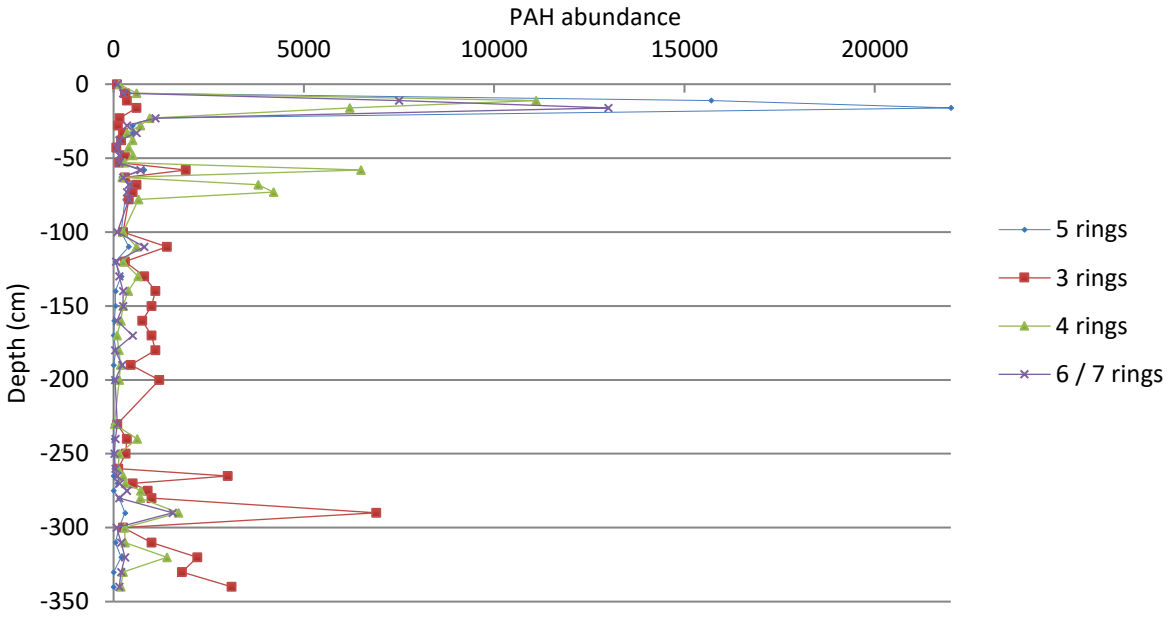

Figure 17: PAH abundances, divided in groups according to their number of aromatic ring systems.

Abundances of PAHs with same number or ring systems summed up as follows: Phenanthrene, Methylphenanthrene, Dimethylphenanthrene and Dimethylphenanthracene (red line), Fluoren, Pyren, Methylfluoranthene, Methylpyrene, Chrysen, Triphenylene and Benzo(a)anthracene (green line), Benzofluoranthene, Benzopyrene, Perylene, Methylbenzofluoranthene and Methylbenzopyren (blue line), Anthanthrene and Coronene (purple line).

In the lowest meter of the profile, an increase of especially LMW PAHs is indicated. PAH concentrations decrease and vary with decreasing depth until 1.2 m, and throughout the profile most PAHs slightly vary until 100 cm depth. Afterwards, a considerable increase of PAH abundances is visible, peaking in depths of 73 to 58 cm. In depths of 53 to 33 cm, PAHs are comparably low, before increasing to maximum values in a depth of 16 cm, what is especially revealed with PAHs of higher numbers of aromatic ring systems and thus HMW PAHs.

4. Discussion and interpretation

The aim of this master thesis was to detect patterns in lipid distributions and link them to anthropogenic and natural changes in the last 4500 years. The thesis focussed on climatic factors such as precipitation, temperature and peat water level but also on predominant vegetation changes. The most relevant results are discussed with regard to the research questions. Where possible, correlations between different molecular information were made and afterwards linked to climatic or anthropogenic components. If it is assumed, that deeper layers of the peat correspond to a larger time period, what is caused by compression of layers and further decomposing processes due to older age, an increase of layer thickness corresponded to shorter time intervals with increasing depth can be suggested (Fig.18). Time periods are named according to Musa Bandowe et al. (2014).

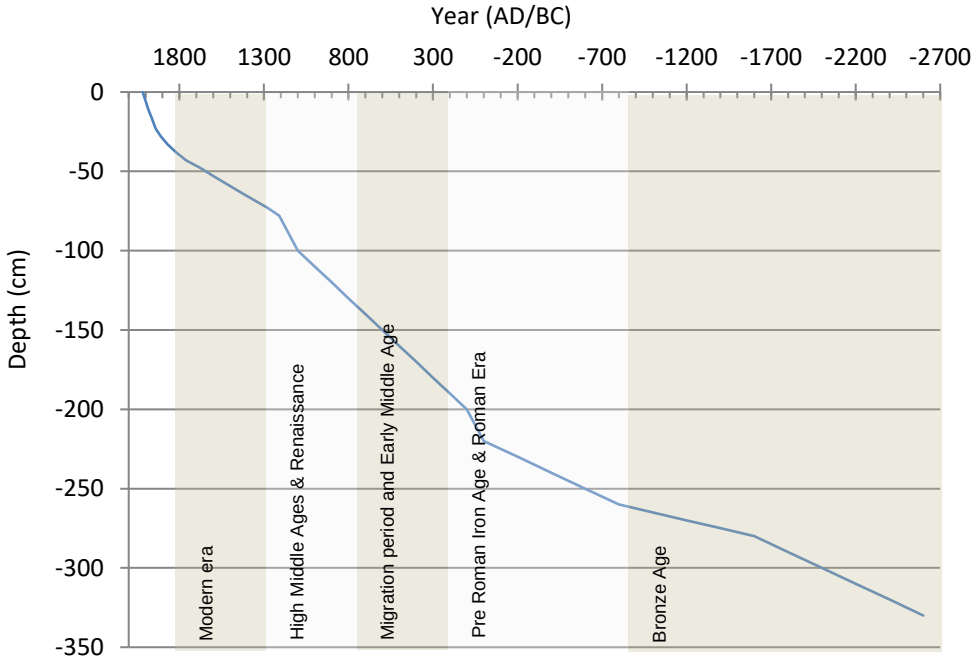

Figure 18: Suggested age of different peat layers

Periods named according to Musa Bandowe et al. (2014) and hereafter used as eras for setting in context the results of this master thesis. Age of peat (blue line)

It is expected, that distributions of lipids (*n*-alkanes, *n*-alcohols, and *n*-fatty acids) in the Beerberg peat changed through time, triggered by a change of contributing plant species and variations in climate. If and how climate and vegetation around the Beerberg peat have changed in the last 4500 years, will be discussed in the following section.

4.1 Vegetation reconstruction

In order to succeed in reconstructing past vegetation, it is crucial to know where the biomass input originates from. Biomarkers from different biological origins have different CPI_{alk} values (Zheng et al., 2007). As Zheng et al. (2007) mention, *n*-alkanes of cuticular waxes of high plants have CPI values >5, whereas bacteria and algae show lower CPI values. As all CPI_{alk} values of the Beerberg peat are higher than 5, input from bacteria and algae can be excluded (Fig. 11).

Indicators, which give a first idea about the predominant vegetation, are the relative proportions of certain *Sphagnum* sp. or other plants. C_{23} and C_{25} alkanes have a rather similar trend (Fig. 20, App.), and by chance they both are indicative for dominant *Sphagnum* sp. This means, that in depths where high abundances of the two *n*-alkanes occur, *Sphagnum* sp. may have been the predominant vegetation. At depths with lower C_{23} and C_{25} alkane abundances, C_{29} and C_{31} alkane abundances increase, what points to a change of predominant vegetation, as C_{31} alkane is characteristic for woody and herbaceous plants and C_{29} alkane for shrubs such as *Calluna* sp. This can be due to possible releases of long-chain alkanes during peat decomposition (Zhang et al., 2017). Detected shifts are especially visible in depths of 270 cm (corresponds to Bronze age) and approximately 78 cm (corresponds to Middle Ages & Renaissance) with *Sphagnum* sp. being predominant in layers between 250 and 100 cm. Thus, alternating changes of vegetation are to be expected. Baas et al. (2000), Ficken et al. (1998), Sever et al. (1972) and Nott et al. (2000) used these indicators for reconstructing vegetation in their papers.

The *n*-alkane P_{aq} ratio additionally provides information about predominant vegetation. Temporal changes in P_{aq} can result from fluctuation in Sphagnum contributions with high P_{aq} values during *Sphagnum* sp. dominated stages (Zhang et al., 2017). As already mentioned it is the relative abundance of *Sphagnum* sp. over other bog-forming plants. Additionally, high P_{aq} ratios indicate a rather Sphagnum dominated phase. P_{aq} values form three clusters (Fig. 10) . The first cluster with lower P_{aq} values in deep layers, which correspond to the Bronze Age, indicates a predominance of bog-forming plants other than *Sphagnum* sp. In the second cluster, corresponding to the pre Roman Iron Age and Roman Era with higher ratios, a Sphagnum dominated phase is indicated, before changing back to a predominance of other plants in higher layers (Migration period, Early Middle Age and Modern Era). Surprisingly, this correlates with

the above mentioned abundances of different *Sphagnum* sp. Especially C_{23} is the dominant alkane in layers (Fig. 20, App.), where P_{aq} values are high and C_{31} and C_{29} abundances are comparably low. This is especially visibe in layers from 250 to 100 cm, which are related to the Iron Age, Roman Era and Early Middle Age.
Baas et al. (2000) and Zhang et al. (2017) mention a domination of C_{24} and C_{26} fatty acids, which occurred in two Sphagnum species and this was verified with the available data from the Beerberg peatland (Fig. 21, App.). Indeed, C_{24} and C_{26} *n*-fatty acid proportions are higher in before detected Sphagnum dominated phases.
This indicates that C_{24} *n*-fatty acid is also an effective biomarker for Sphagnum as suggested by Pancost et al. (2002) and (Nichols et al., 2009). Moreover, this is in agreement with Karunen and Salin (1980) and Ficken et al. (1998), who used specific fatty acids as biomarkers for Sphagnum dominated stages.

n-alcohols occur in a range of C_8 – C_{35} in samples of the Beerberg peat. Ficken et al. (1998) found a domination of C_{24}, C_{26} and some cases C_{28} alcohol in fresh *Sphagnum* sp. Compared to the results of certain alkanes being indicative for *Sphagnum* sp., the patterns of C_{24} and C_{26} alcohols should be expectedly similar to the abundances of C_{23} and C_{25} alkanes. C_{24} and C_{26} alcohol undeniably have a similar trend (Fig. 22, App.). Other than C_{28} alcohol, they peak in depths, which were before detected as *Sphagnum* sp. dominated stages. The course of the C_{28} alcohol is reversed and will thus be excluded from the interpretation. Baas et al. (2000) mention, that only in some cases C_{28} alcohols were dominant in Sphagnum species, as the distribution is more variable than from C_{24} and C_{26}. alcohols A dominance of C_{24} and C_{26} alcohols in Sphagnum dominated stages is in great agreement with Zhang et al. (2017).

4.2 Climate reconstruction

Further ratios of lipids can help to underline the findings so far and link vegetation changes to climatic variations in the past. In the following section, the climatic factors humidity, precipitation and temperature are examined in detail.

Humidity

Mäkilä and Saarnisto (2008) analysed impacts of climate variations on boreal peatlands during Holocene. One of their findings is that shrub growth is favoured when water tables are lowered, whereas sedges and herbaceous species are more

productive with water tables at the peat surface. This hypothesis can be transferred to the Beerberg peat and can be assessed by total carbon and nitrogen concentrations, combined with $\delta^{13}C$ isotope values.

Total carbon and total nitrogen concentrations follow a similar trend (Fig. 3 and 4), as shifts in concentrations occur in comparable depths (especially 260 cm, 50 cm, 30 cm and 11 cm). This could be linked to changing moisture. As Mäkilä and Saarnisto (2008) found out, the degree of humification is lower during moist and cool periods, what is a result of lower decomposition rates. This leads to an increased carbon accumulation and thus to higher total carbon contents. On the other hand, warmer and drier temperatures lead to drying peatlands and thus to lower carbon contents, as more carbon is released.

Furthermore, nitrogen is sequestered in peatlands with the accumulating organic matter (Verhoeven et al., 1990). Where microbial decomposition is present, nitrogen values are low, as nitrogen is being released. Therefore, nitrogen accumulation is high where microbial decomposition is hindered, what normally is in anaerobic conditions. Linked to moisture this means that moist conditions lead to high N values and dry conditions to low N values. The detected shifts in C and N values may indicate that there must have been a change in climate. In phases where C values decrease, the climate may have changed towards a drier and warmer climate, whereas increasing values point to a change towards cooler and wetter climate. Increasing N values mean a change to more moist weather, whilst decreasing values mean drier environmental conditions.

The reason for this phenomenon can be explained by the following cycle: Higher temperatures lead to increased evapotranspiration, what means that water is evaporated from the peatland. As a result, the water table shrinks, what reduces soil moisture. As a consequence, decomposition rates increase, whereas less carbon is accumulated in the peat. Transferred to the Beerberg peat, alternating variations between dry, warm and cool, wet climate indicate changed climatic conditions in the past (Fig. 3 and 4). From a depth of 350 cm, C and N concentrations decrease until reaching a depth of approximately 250 cm. This indicates a change to dry and warm climate during the Bronze Age. Afterwards, as the C concentrations remain more or less stable with increasing depth and N concentrations increase, a shift to moister climate is expectable, what corresponds to times of the pre Roman Iron Age and Roman Era. Subsequently, a short decrease of both concentrations at a depth of 50

cm followed by an increasing period in higher depths indicate a short-term change in climatic conditions during the Modern Era. This correlates with the in the previous section gathered results: *Sphagnum* sp. prefer moist or wet conditions, thus, they may have been predominant in periods, where C and N values are increasing, what corresponds to depths between 250 and 100 cm and to the pre Roman Iron Age and Roman Era as well as the Early Middle Ages.

Other molecular proxies for moisture are the proportions of C_{23} and C_{29} alkanes. During dry periods, *Sphagnum* sp., with no vascular system, are unable to take advantage of the available water at the lowered water table, and its growth is impeded. Consequently, vascular plants contribute a greater proportion of leaf waxes to the peat deposited during drier times. Therefore, changes in the amount of C_{23} and C_{29} *n*-alkanes, the most abundant alkanes in *Sphagnum* sp. and vascular plants respectively, reflect changes in moisture balance. Higher C_{23} abundances indicate more contribution by *Sphagnum* sp. and thus, wetter conditions during the time of deposition (Nichols et al., 2009). Unfortunately, this statement cannot completely be confirmed with measured C_{23} and C_{29} *n*-alkane proportions (Fig. 20, App.). Although the trends of the two graphs are more or less contrarious, as expected, the Sphagnum dominant phases do not fully overlap the detected moist phases (Fig. 3 and 4). This is only true for depths between 200 and 70 cm. Moreover, near the peat surface, carbon and nitrogen concentrations indicate that dry and warm climate was present, what C_{23} and C_{29} alkane proportions confirm. This means that other peat-forming plants were predominant in recent years, as the C_{23} alkane proportion declines and C_{29} alkane increases in the upper 20 cm of the profile.

Precipitation

In order to underline the findings achieved so far, an approach of Zhang et al. (2014) can be consulted. One of the main observations of their paper is that $\delta^{13}C$ isotope values of plants in peat bogs are sensitive to variation in humidity. They found out, that more precipitation leads to higher $\delta^{13}C$ isotope values. Increasing compositions with increasing depth in the lower 1.5 m (Bronze Age) of the Beerberg peatland indicate a shift towards enhanced precipitation (Fig.7). Between depths of 200 cm and 100 cm (pre Roman Iron Age and Renaissance and Migration Period and Early Middle Ages), $\delta^{13}C$ isotope compositions remain high, what suggests a wetter period, which favours

growth of *Sphagnum* sp. Declining isotope compositions between 100 cm and 50 cm (Middle Ages and Renaissance) point to a change of precipitation towards drier conditions, followed by a re-increase at a depth of 50 cm, implying a recurring raise of precipitation. This supports the above mentioned statements resulted from C and N concentrations as well as the fact that *Sphagnum* sp. prefer wet conditions, as shifts occur in comparable depths and point towards similar directions.

Temperature

A method to check this observation is the consultation of *n*-lipid CPI and ACL ratios. Zhang et al. (2014) and Zheng et al. (2007) verify, that a lower CPI_{alk} value and higher ACL_{alk} value indicate a warmer climate, whereas higher CPI_{alk} and lower ACL_{alk} suggest colder conditions. This can be explained by the fact that a cold and dry climate leads to slow microbial degradation and diagenesis. On the other hand, wet and warm climatic conditions enhance microbial degradation and alteration of organic matter (Zheng et al., 2007). Transferred to the Beerberg peat this means, that in deeper layers, which correspond to the Bronze Agea and where low CPI_{alk} and high ACL_{alk} values occur, a rather warm climate is suggested (Fig. 11 and 9). At a depth of approximately 240 cm CPI_{alk} values start to increase and ACL_{alk} values start to decrease with increasing depth, what indicates a shift towards colder climate. This is supported by the results of this thesis mentioned context of C and N contents, where a shift towards colder climate in the same depth was detected. A next shift is visible in a depth of 150 cm (Migration Period and Early Middle Ages), where ACL_{alk} values increase and indicate a shift towards moister and wetter climatic conditions. In a depth of 50 cm, CPI_{alk} values are still increasing, what again indicates a shift towards colder climate conditions. Similar observations were made with results of ACL_{FA} values (Fig. 13) as well as with CPI_{FA} values (Fig.12). In the lower meter of the profile (Bronze Era), values are low and with increasing depth the values increase until a depth of 250 cm (pre Roman Iron Age and Roman Era). Around 100 cm (Middle Ages & Renaissance), the peak is reached and then then the values start to decrease with increasing depth until 50 cm, what suggests a shift towards warmer climatic conditions. Unfortunately, ACL_{alc} and CPI_{alc} values do not confirm these observations. Althouh both graphs (Fig. 15 and 16) show shifts in depths of 250 and 100 cm, trends are not as clear as in the other values.

Another method to confirm these findings is the approach of Zhou et al. (2004), who link fatty acids to temperature. They found out, that $C_{16:1}/C_{16:0}$ and $C_{18:1}/C_{18:0}$ are indicators for palaeotemperature: Low values of the ratios correspond to higher temperatures, what Zhou et al. (2004) confirmed with pollen data. Regarding the Beerberg peatland, $C_{16:1}/C_{16:0}$ values are low in depths of 320 – 250 cm (Bronze Age), 200 – 150 (pre Roman Iron Age and Roman Era) and 15 – 30 cm (Modern Era), what suggests warmer climatic phases during time of evolvement of the peatland (Fig. 14). In general, results show that the $C_{16:1}/C_{16:0}$ and $C_{18:1}/C_{18:0}$ ratios are rather low with some exceptions and that they vary frequently, what indicates short-term variations of temperature. According to $C_{18:1}/C_{18:0}$ results (Fig. 23, App.), values are higher in layers between 50 and 100 cm (Middle Ages and Renaissance) and in upper layers (Modern Era), what indicates the shifts towards colder conditions, already detected and discussed in previous sections. This can be explained by diagenetic degradation. The low values indicate that diagenetic degradation of the unsaturated acids has been severe in the sequence and the fluctuations may indicate that the amount of degradation of these biomarkers has indeed been very sensitive to climatic conditions. Thus, they are hence an indicator for palaeotemperature changes.

Anthropogenic impacts

In context of the Beerberg peatland different concentrations of PAHs were found (Fig. 17). In a depth of 275 cm (Bronze Age) comparably high concentrations of PAHs were found. As already stated, the Beerberg peat has an approximate age of 4500 years. Higher PAH concentrations in deeper layers may be traced back to the “Schönfelder” culture, an archaeological culture group of the Neolithic Age in Germany which lived from 2900 BC to 2100 BC (Behm-Blancke, 1967). They dispersed in the Elbe-area from Wendland to Bohemia, whilst the Beerberg peat lies in this region. Schönfelder people were one of the first folks who undertook cremation burials. In later ages, pits of Schönfelder culture were found whilst mining (Behm-Blancke, 1967). As the population survived and lived in the Thuringian area for eight centuries, this could probably be the reason why PAH concentrations are higher in great depths of the Beerberg peat. Another possible reason is the migration of light-fraction PAHs such as phenanthrene, fluoranthene, pyrene or chrysene into deeper layers (Gabov et al., 2007). Heavier PAHs like benzo(a)pyrene usually stay in higher layers and are accumulated in the upper organic horizons.

The next increase of PAHs is visible in a depth of 58 – 78 cm, which corresponds to to times during Middle Ages and Renaissance. This could be linked to regional iron production (Musa Bandowe et al., 2014). Van der Meulen (2008) mentions in his thesis, that Thuringia was the core area for iron production in the Iron Age, as it lies near iron repositories. This could be a reason for increased PAHs, although the Iron Age took place a bit earlier. Here the hypothesis of light PAHs being migrated to deeper layers could also be a possibility.

A sharp increase of PAH concentrations is visible in depths of 11 to 23 cm (Modern Era). During the 15th and 19th century, the Little Ice Age took place. This period is characterized by rather few solar activity and increased volcanic activity. The highest values correspond to the Modern Era and in the 18th century Industrial Revolution started. Musa Bandowe et al. (2014) state, that Perylene (m/z 252), a mainly biologically produced compound, was the dominant PAH in pre-industrial times. PAHs with a molecular mass of 252 have high abundances in depths of 23 – 38 cm. With this it gets clear, that the depths of 11 – 23 cm have been developed during industrialization, which mainly took place in the 19th century. The invention of steam engines, unlocking of coal deposits and trains led to high emissions of PAHs. This is strongly supported by other studies, carried out in different areas of the world, such as Canada (Dreyer et al., 2005), China (Liu et al., 2012) and Europe (Fernandez et al., 2000).

5. Conclusion

As a natural process, vegetation is typically affected by climate changes, as response to changing environmental conditions. Regarding the Beerberg peat, alternating predominant vegetation reflects past climatic conditions (Fig. 19). A dominance of *Sphagnum* sp. can especially be detected in depths of 275 – 250 cm, 170 – 130 cm and 68 – 58 cm. The Verhib model with output below enables a reconstruction of vegetation, which was present on the peat surface during evolvement of the Beerberg peat. This helps to underline the findings so far.

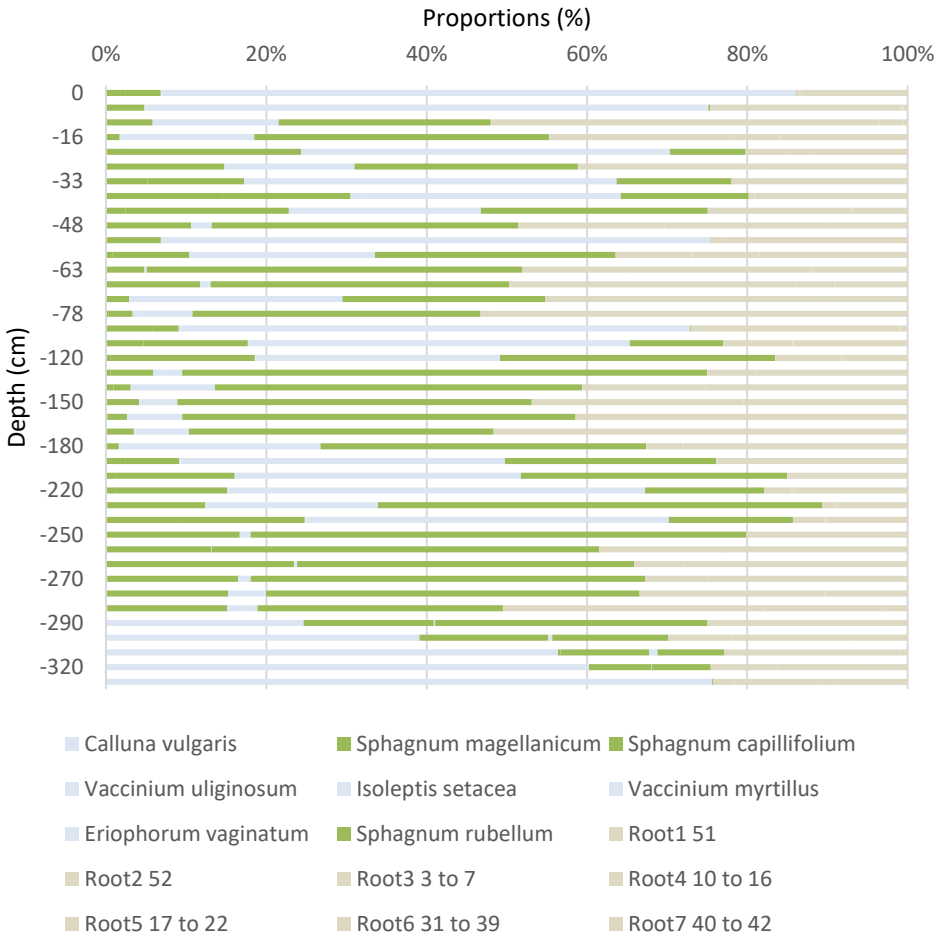

Figure 19: Overview of modelled vegetation during evolvement of the peat bog.

Sphagnum species (green bars), belowground biomass (brown bars), vegetation other than *Sphagnum* species (light blue bars). Tab. 2 App. for exact depths

Many indicators point to minor or major changes of palaeoclimatic factors such as precipitation, humidity and temperature. Especially in depths of 250 and 100 cm strong

shifts were detected. In the following section these shifts are set in context to past climatic history and summed up.

During the Bronze Age, which took place from approximately 2700 BC until 600 BC and corresponds to peat depths of 350 cm to 250 cm, numerous parameters such as CPI_{alk}, CPI_{FA}, ACL_{alk}, $C_{16:1}/C_{16:0}$ fatty acid ratio and $\delta^{13}C$ isotope values indicate a change from cold and wet to warm and dry climate. Results of this thesis show, that in the oldest layers of the Beerberg peat, plant species other than *Sphagnum* were primarily predominant. This statement is supported by the Verhib modelling. As visible in the figure, *Sphagnum* sp. were not the predominant vegetation in the lower layers (Fig. 19). Especially *Calluna vulgaris* was present in the lower half meter of the profile. In a depth of 250cm, which corresponds to the end of the Bronze Age, an increase of Sphagnum is suggested.

This era is followed by the pre Roman Iron Age and Roman Era (approx. 600 BC to 500 AD, peat depths 250 cm to 150 cm). $\delta^{13}C$ isotope compositions and P_{aq} ratios indicate, that peat evolved during this time has been affected by enhanced precipitation, which favoured growth of *Sphagnum* sp. This is supported by the results of the Verhib modelling, as it gets clear that in depths corresponding to the End of the Roman Era, a domination of Sphagnum is indicated. In the course of time, the dry and warm climate changed to rather moist and cold conditions, as indicated by $C_{16:1}/C_{16:0}$ fatty acid ratio, ACL_{alk} and CPI_{alk}. The Verhib modelling support this statement, as Sphagnum proportions start to increase in a depth of approximately 180 cm with decreasing depth.

The Migration Period and Early Middle Ages, which took place from 500 AD to 1000 AD and corresponds to a depth of 150 cm to 100 cm is distinguished through moist and cold climate with a shift to even colder climatic conditions with increasing depth. $\delta^{13}C$ isotope compositions, ACL_{alk} and CPI_{alk} as well as N and C values indicate major changes in climate with *Sphagnum* sp. as the predominant vegetation. Musa Bandowe et al. 2014) observed similar changes in times of Migration Period and Early Middle Ages and state, that in response to colder and wetter conditions, human activity was reduced during these times. Very low PAH abundances occur in these depths of the Beerberg peat, what underline the statement of Musa Bandowe et al. (2014). The

alternation between *Sphagnum* sp. and other peat forming plants is visible in depths corresponding to the Migration Period and Early Middle Ages.

In times of Middle Ages and Renaissance (1000 AD to 1600 AD and depths from 100 cm to 50 cm) short term climatic changes are indicated through a shift to warmer conditions ($\delta^{13}C$, CPI_{FA}), followed by a shift to colder conditions (fatty acid $C_{18:1}/C_{18:0}$). The colder conditions might reflect the beginning of the little ice age, which is a recent period of colder climatic conditions from 16th to 19th century (Mann, 2002).

In the Modern Era (1600 until present), corresponding to peat depths of 50 cm to peat surface, PAH abundances are very high and alternating shifts from warmer to colder conditions occur. ACL_{FA} and CPI_{alk} ratios argue for a shift to rather cold and moist conditions, whereas fatty acid $C_{16:1}/C_{16:0}$, $\delta^{13}C$ isotope values, C and N concentrations indicate a change towards dry and warm climate. This is also supported by the Verhib modelling (Fig. 19). It is not clear which plants were predominant. Thus, short term climatic changes were likely in the last 500 years.
Additionally, high PAH concentrations can be traced back to industrialization. Moreover, concentrations decreased in the last 11 cm to pre-industrial levels because of emission control measurements and the switch from coal to oil and gas as major fuel sources. This is also supported by Musa Bandowe et al. (2014). Nevertheless, a shift to warmer conditions during the last years is clearly measurable and is most certainly linked to climate warming.

6. Limitations

Low-molecular weight alkanes are for example much more abundant in some plants than others, thus, the lipid distributions vary amongst different types of plants. Moreover, yields of lipids from *Ericaceae* sp. are much higher than from *Sphagnum* sp. (Pancost et al., 2002). Yields were, however, not measured in context of this master thesis. In order to expand or review the results of this thesis, further analyses such as the measuring of yields would have been helpful. Thus, some uncertainties in the results must be assumed.

Moreover, Zhang et al. (2017) mention that the fatty acid and alcohol distributions also seem to be rather characteristic for reconstructing vegetation or climate changes. However, their distribution is not distinct enough from those of other higher plants to be of use in tracing Sphagnum inputs. Another limitation is the fact that fatty acids and alcohols could be reduced to alkanes in anoxic environments, what leads to uncertainties or modified results.
However, a broad overview of vegetation and climate changes in the last 4500 years has already been given.

7. Outlook

Regarding the potential of future climate warming, peatland drying will likely occur. This will affect peat carbon sequestration and lead to increased release of carbon instead of carbon fixation. In turn, the carbon balance will be affected, in worst cases, on hemispheric scale. Another impact of climate change may be an induced water table drawdown, which may lead to shifts of vegetation communities in response to shifting moisture conditions. Depending on the extent of drying, peatland vegetation will maybe respond with enhanced growth of shrubs and trees. Thus, it is crucial to continue to do research of peatlands and to evolve new methods perpetually.

8. References

- Abdel-Shafy, H.I and Mansour, M.S.M. (2016). A review on polycyclic aromatic hydrocarbons: Source, environmental impact, effect on human health and remediation. *Egyptian Journal of Petroleum 25*(1), 107 – 123.
- Baas, M., Pancost, R., van Geel, B., Sinninghe Damsté, J.S. (2000). A comparative study of lipids in *Sphagnum* species. *Organic Geochemistry 31*, 535 – 541.
- Beetz, S. (2008). Geoökologische Erfolgskontrolle der Renaturierung von Mooren des Thüringer Waldes. Diploma thesis in Geography, Department of Geography, University of Jena.
- Behm-Blancke, G., Bach, H., Bach, A. (1967). Zum Problem der schnurkeramischen Leichenverbrennung in Thüringen. *Alt-Thüringen Jahresschrift des Museums für Ur- und Frühgeschichte Thüringen*, 9. Band, 225 – 255.
- Belyea, L.R. and Malmer, N. (2004). Carbon sequestration in peatland: patterns and mechanisms of response to climate change. *Global Change Biology 10(7)*, 1043 – 1052.
- Bezabeh, D., Jones, D.A., Ashbaugh, L.L., Kelly, P.B. (1999). Screening of aerosol filter aamples for PAHs and nitro-PAHs by laser desorption ionization TOF mass spectrometry. *Aerosol Science and Technology 30*(3), 288 – 299.
- Blytt, A. (1876). Essay on the immigration of the Norvegian flora during alternating rainy and dry periods. Kristiana, Cammermeyer.
- Bojakowska, I. and Sokolowska, G. (2003). Polycyclic Aromatic Hydrocarbons in materials of burned peatlands. *Polish Journal of Environmental Studies 12(4),* 401 – 408.
- Chambers, F.M. and Charman, D.J. (2004). Holocene environmental change: Contributions from the peatland archive. *The Holocene 14(1)*, 1 – 6.
- Clymo, R.S. (1998). Sphagnum, the peatland carbon economy, and climate change. *Bryology for the Twenty-first Century*, 361 – 368.
- Dreyer, A., Radke, M., Turunen, J., Blodau, C. (2005). Long-term change of Polycyclic Aromatic Hydrocarbon deposition to peatlands of Eastern Canada. *Environmental Science & Technology 39,* 3918 – 3924.

- El Nemr, A., Said, T.O., Khaled, A., El-Sikaily, A., Abd-Allah, A.M.A. (2007). The distribution and sources of Polycyclic Aromatic Hydrocarbons in surface sediments along the Egyptian Mediterranean coast. *Environmental Monitoring & Assessment 124*, 343 – 359.
- Fernandez, P., Vilanova, R.M., Martinez, C., Appleby, P., Grimalt, J.O. (2000). The historical record of pyrolic pollution over Europe registered in the sedimentary PA from remote mountain lakes. *Environmental Science & Technology 34,* 1906 – 1913.
- Ficken, K.J., Barber, K.E., Eglinton, G. (1998). Lipid biomarker, $\delta^{13}C$ and plant macrofossil stratigraphy of a Scottish montane peat bog over the last to millennia. *Organic Geochemistry 28,* 217 – 237.
- Firbas, F. (1949). Spät- und nacheiszeitliche Waldgeschichte Mitteleuropas nördlich der Alpen. Band. 1: Allgemeine Waldgeschichte, Jena.
- Fischer, K. (2008). Das Beerbergmoor. Thüringer Naturbrief, http://www.thueringer-naturbrief.de, accessed on 15.5.17
- Gabov, D.N., Beznosikov, V.A., Kondratenok, B.M. (2007). Polycyclic aromatic hydrocarbons in background podzolic and gleyic peat-podzolic soils. *Eurasian Soil Science 40(3),* 282 – 291.
- Gore, A.J. (1983). Introduction. In: Gore, A.J., editor, Ecosystems of the world 4B mires: swamp, bog, fen and moor general studies, Amsterdam, Elsevier, 1 – 34.
- Heinselman, M.L. (1970). Landscape evolution, peatland types and the environment in the Lake Agassiz peatlands natural area, Minnesota. *Ecological Monographs 40(2),* 235 – 261.
- Hellmuth, E. (2006). Besucherzählungen mit Lichtschranken im Biosphärenreservat Vessertal-Thüringer Wald. In: Besuchermonitoring und ökonomische Effekte in Nationalen Naturlandschaften, Biosphärenreservat Vessertal-Thüringer Wald Verwaltung (Editor), Satz- und Druck Centrum Saalfeld GmbH, Schmiedefeld am Rennsteig, Germany.
- Huang, X., Wang, C., Zhang, J., Wiesenberg, G.L.B., Zhang, Z., Xie, S. (2011). Comparison of free lipid compositions between roots and leaves of plants in the Dajiuhu Peatland, central China. *Geochemical Joural 45*, 365 – 373.
- Jansen, B., Nierop, K.G.J., Hageman, J.A., Cleef, A.M., Verstraten, J.M. (2006). The straight-chain lipid biomarker composition of plant species responsible for

the dominant biomass production along two altitudinal transects in the Ecuadorian Andes. *Organic Geochemistry 37*, 1514 – 1536.

- Jansen, B. and Wiesenberg, G.L.B. (2017). Opportunities and limitations related to the application of plant-derived lipid molecular proxies in soil science. Manuscript under review for journal SOIL.
- Karunen, P. and Salin, M. (1980). Lipid composition of Sphagnum fuscum shoots of various ages. *Finnish Chemistry 7,* 500 – 502.
- Lange, E. (1967). Zur Vegetationsgeschichte des Beerberggebietes im Thüringer Wald. *Feddes Repertorium 76(3)*, 205 – 219.
- Lerda, D. (2011). Polycyclic Aromatic Hydrocarbons (PAHs) Factsheet. 4th edition, European Commission, Joint Research Centre, Institute for Reference Materials and Measurements.
- Liu, L., Wang, J., Wei, G., Guan, Y., Wong, C.S., Zeng, E.Y (2012). Sediment records of Polycyclic Aromatic Hydrocarbons (PAHs) in the continental shelf of China: Implications for evolving anthropogenic impacts. *Environmental Science & Technology 46,* 6497 – 6504.
- Malawska, M., Ekonomiuk, A., Wilkomirski, B. (2006). Polycyclic aromatic hydrocarbons in peat cores from southern Poland: distribution in stratigraphic profiles as an indicator of PAH sources. *Mires and peat 1(05),* 1 – 14.
- Mäkilä, M. and Saarnisto, M. (2008). Carbon accumulation in boreal peatlands during the Holocene – Impacts of climate variations. In: Peatlands and climate change, M. Strack (Editor). International Peat Society, Saarijärven Offset Oy, Jyväskylä, Finland.
- Mann, M.E. (2002). Little Ice Age. The Earth system: physical and chemical dimensions of global environmental change. In: Encylopedia of Global Environmental Change, 504 – 509.
- Musa Bandowe, B.A., Srinivasan, P., Seelge, M., Sirocko, F., Wilcke, W. (2014). A 2600-year record of past polycyclic aromatic hydrocarbons (PAHs) deposition at Holzmaar (Eifel, Germany). *Palaeogeography, Palaeoclimatology, Palaeoecology 401*, 111 – 121.
- Nichols, J.E., Booth, R.K., Jackson, S.T., Pendall, E.G., Huang, Y. (2006). Palaeohydrologic reconstruction based on n-alkane distributions in ombrotrophic peat. *Organic Geochemistry 37,* 1505 – 1513.

- Nichols, J.E., Walcott, M., Bradley, R., Pilcher, J., Huang, Y. (2009). Quantitative assessment of precipitation seasonality and summer surface wetness using ombrotrophic sediments from an Arctic Norwegian peatland. *Quarternary Research*, DOI 10.1016/j.yqres.2009.07.007
- Nott, C.J., Xie, S., Avsejs, L.A., Maddy, D., Chambers, F.M., Evershed, R.P. (2000). n-alkane distributions in ombrotrophic mires as indicators of vegetation change related to climatic variation. *Organic Geochemistry 31*, 231 – 235
- Pancost, R.D., Baas, M., van Geel, B., Sinnighe Damsté, J.S. (2002). Biomarkers as proxies for plant in puts to peats: an example from a sub-boreal ombrotrophic bog. *Organic Geochemistry 33*, 675 – 690.
- Schellekens, J. and Buurman, P. (2011). n-Alkane distributions as palaeoclimatic proxies in ombrothrophic peat: The role of decomposition and dominant vegetation. *Geoderma 164*, 112 – 121.
- Sernander, R. (1908). On the evidence of postglacial changes of climate furnished by the peat-mosses of northern Europe. *Geologiska Föreningen i Stockholm Förhandlingar 30*, 467 – 478.
- Sever, J.R., Lytle, T.F., Haug, P. (1972). Lipid geochemistry of a Mississippi coastal bog environment. *Contributions to Marine Sciences 16,* 149 – 161.
- Thuens, S., Blodau, C., Radke, M. (2013). How suitable are peat cores to study historical deposition of PAHs? *Science of the Total Environment 450 – 451*, 271 – 279.
- Van der Meulen, M. (2008). Anthropogene Einflüsse auf das Relief in landwirtschaftlich geprägten Räumen am Beispiel des Kulturlandschaftswandels in Thüringen bis 1900. Bachelor thesis, Ruhr-University, Bochum.
- van Verhoeven, J.T.A., Maltby, E., Schmitz, M.B. (1990). Nitrogen and phosphorus mineralization in fens and bogs. *Journal of ecology 78,* 713 – 726.
- Wagner, S. (2013). Analysis of peat decomposition, element distribution patterns and element output of two peat bogs in the Thuringian Forest. Master Thesis in Geoecology-Environmental Sciences, Department of Hydrology, Universität Bayreuth.
- Wang, X., Huang, X., Sachse, D., Ding, W., Xue, J. (2016). Molecular palaeoclimate reconstructions over the last 9 ka from a peat sequence in South China. PLoS ONE 11(8): e0160934. DOI: 10.1371/journal.pone.0160934.

- Wiesenberg, G.L.B. and Gocke, M.I. (2015). Analysis of Lipids and Polycyclic Aromatic Hydrocarbons as Indicators of Past and Present (Micro)Biological Activity. In: T.J. McGenity et al. (eds.), Hydrocarbon and Lipid Microbiology Protocols, Springer Protocols Handbooks, DOI 10.1007/8623_2015_157, Springer Verlag, Heidelberg.
- Wiesenberg, G.L.B. and Schwark, L. (2006). Carboxylic acid distribution patterns of temperate C_3 and C_4 crops. *Organic Geochemistry 37,* 1973 – 1982.
- Zhang, Y., Zheng, M., Meyers, P.A., Huang, X. (2017). Impact of early diagenesis on distribution of Sphagnum n-alkanes in peatlands of the monsoon region of Chia. *Organic Geochemistry 105,* 13 – 19.
- Zhang, Y., Liu, X., Lin, Q., Gao, C., Wang, J., Wang, G. (2014). Vegetation and climate change over the past 800 years in the monsoon margin of northeastern China reconstructed from n-alkanes from the Great Hinggan Mountain ombrotrophic peat bog. *Organic Geochemistry 76*, 128 – 135.
- Zheng, Y., Zhou, W., Meyers, P.A., Xie, S. (2007). Lipid biomarkers in the Zoigê-Hongyuan peat deposit: Indicators of Holocene climate changes in West China. *Organic Geochemistry 38*, 1927 – 1940.
- Zhou, W., Xie, S., Meyers, P.A., Zheng, Y. (2005). Reconstruction of late glacial and Holocene climate evolution in southern China from geolipids and pollen in the Dingnan peat sequence. *Organic Geochemistry 36,* 1271 – 1284.

9. Appendix

Table 1: Masses of specific PAHs determined

m/z	Name	m/z	Name
178	Phenanthrene, Anthracene	**242**	Methylchrysene, Methyltriphenylene, Methyl-Benzo(a)antracene
192	Methylphenanthrene	**252**	Benzofluoranthene, Benzopyrene
206	Dimethylphenanthrene, Methylphenanthrene, Methylanthracene	**266**	Methylbenzofluoranthene, Methylbenzopyrene
202	Fluoranthene, Pyrene	**276/ 278**	Anthanthrene
216	Methylfluoranthene, Methylpyrene	**300**	Coronene
228	Chrysene,Triphenylene, Benzo(a)anthracene	**302**	Dibenzopyrene

Table 2: Depths of peat layers, related to belowground biomass samples

Sample n°	Depth (cm)	Sample n°	Depth (cm)
138B16GW01	0 - 6	138B16GW22	150 - 160
138B16GW02	6 - 11	138B16GW23	160 - 170
138B16GW03	11 - 16	138B16GW24	170 - 180
138B16GW04	16 - 23	138B16GW25	180 - 190
138B16GW05	23 - 28	138B16GW26	190 - 200
138B16GW06	28 - 33	138B16GW27	200 - 210
138B16GW07	33 - 38	138B16GW29	220 - 230
138B16GW08	38 - 43	138B16GW30	230 - 240
138B16GW09	43 - 48	138B16GW31	240 - 250
138B16GW10	48 - 53	138B16GW32	250 - 260
138B16GW11	53 - 58	138B16GW33	260 - 265
138B16GW12	58 - 63	138B16GW34	265 - 270
138B16GW13	63 - 68	138B16GW35	270 - 275
138B16GW14	68 - 73	138B16GW36	275 - 280
138B16GW15	73 - 78	138B16GW37	280 - 290
138B16GW16	78 - 83	138B16GW38	290 - 300
138B16GW17	100 - 110	138B16GW39	300 - 310
138B16GW18	110 - 120	138B16GW40	310 - 320
138B16GW19	120 - 130	138B16GW41	320 - 330
138B16GW20	130 - 140	138B16GW42	330 - 340
138B16GW21	140 - 150		

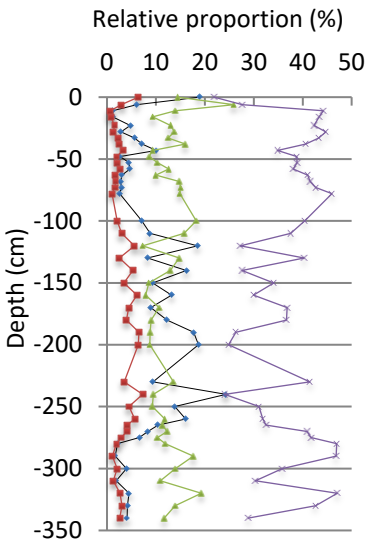

Figure 20: Relative proportions of C_{23}, C_{25}, C_{29} and C_{31} alkanes

C_{25} alkane (blue line), C_{23} alkane (red line), C_{29} alkane (green line), C_{31} alkane (purple line)

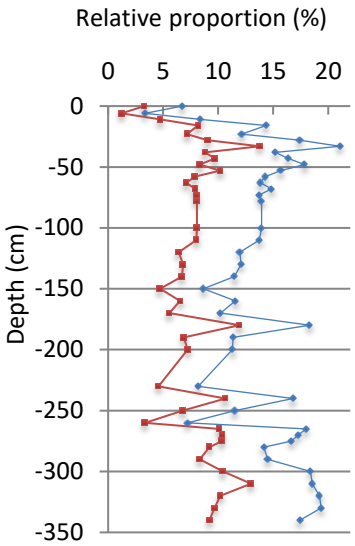

Figure 21: Relative proportions of C_{25} and C_{26} fatty acids

C_{24} fatty acid (blue line) and C_{26} fatty acid (red line)

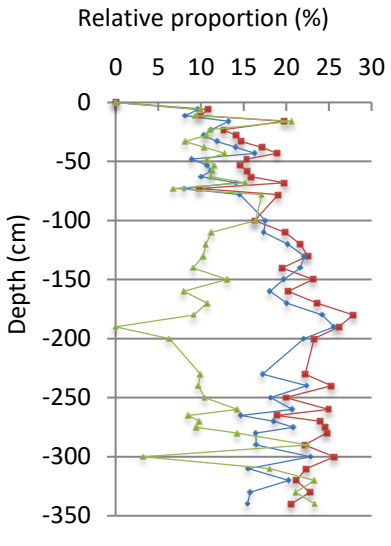

Figure 22: Relative proportions of C_{24}, C_{26} and C_{28} alcohol

C_{24} alcohol (red line), C_{26} alcohol (blue line), C_{28} alcohol (green line)

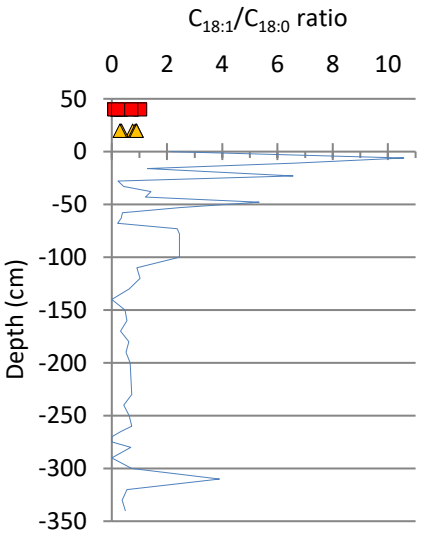

Figure 23: $C_{18:1}/C_{18:0}$ ratios of samples

Blue line (peat), belowground biomass samples (red squares), aboveground biomass samples (orange triangles)

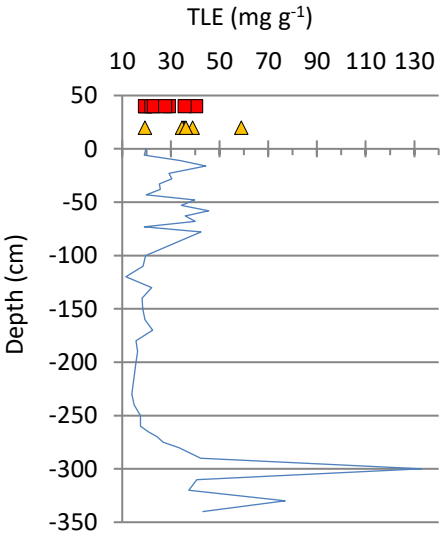

Figure 24: Total lipid extracts in samples.

Blue line (peat), belowground biomass samples (red squares), aboveground biomass samples (orange triangles)

Table 3: *n*-alkanes of samples 1 to 21. Relative abundances of alkanes shown

Sample n°	1	2	3	4	5	6	7	8	9	10	11	12	13	14	15	16	17	18	19	20	21
Upper layer boundary (cm)	0	-6	-11	-16	-23	-28	-33	-38	-43	-48	-53	-58	-63	-68	-73	-78	-100	-110	-120	-130	-140
C17	0.0	0.0	0.0	0.0	0.0	0.0	0.0	0.0	0.0	0.0	0.0	0.2	0.0	0.2	0.3	0.0	0.5	0.2	0.0	0.1	0.4
C18	0.0	0.0	0.0	0.0	0.0	0.0	0.0	0.0	0.0	0.0	0.1	0.3	0.0	0.3	0.2	0.0	0.0	0.0	0.0	0.1	0.3
C19	0.0	0.0	0.0	0.0	0.0	0.0	0.0	0.0	0.0	0.0	0.1	0.7	0.2	0.7	0.5	0.1	0.2	0.2	0.0	0.2	0.4
C20	0.0	0.0	0.0	0.1	0.0	0.2	0.0	0.2	0.0	0.8	0.3	1.6	0.2	1.2	0.8	0.1	0.2	0.2	0.0	0.2	0.5
C21	2.0	3.0	1.1	0.5	0.6	0.7	0.8	0.5	0.8	1.6	0.9	2.9	0.8	2.3	1.7	0.5	0.6	0.6	1.0	0.6	1.1
C22	0.0	0.0	0.2	0.2	0.3	0.3	0.0	0.3	0.5	1.2	0.5	2.0	0.3	1.5	1.4	0.2	0.3	0.5	0.8	0.5	1.2
C23	6.4	3.0	0.7	0.8	1.5	1.3	2.2	2.5	3.3	2.0	2.0	2.6	1.7	1.7	1.6	1.0	2.1	3.0	5.6	2.5	5.3
C24	2.4	1.4	0.3	0.3	0.6	0.4	0.6	0.5	0.8	0.5	0.7	0.5	0.5	0.4	0.5	0.3	0.7	1.0	1.6	1.0	2.4
C25	18.9	6.0	1.2	1.2	4.7	2.9	5.6	7.2	10.1	2.6	4.5	4.7	3.1	2.8	2.9	2.6	7.1	8.8	18.5	8.3	16.2
C26	3.3	2.7	0.7	0.5	0.7	0.5	0.6	0.6	1.6	0.5	0.8	0.5	0.6	0.5	0.5	0.4	0.7	1.0	1.7	1.3	2.5
C27	15.1	10.2	4.1	2.5	4.7	3.7	4.5	5.0	7.6	3.1	4.5	3.9	3.3	3.1	3.1	3.0	6.2	6.6	11.1	5.9	10.1
C28	3.5	4.9	1.3	0.9	1.0	1.1	1.0	0.8	1.2	1.1	1.3	1.1	1.2	0.9	1.3	1.0	1.2	1.5	1.6	1.3	2.0
C29	14.4	25.9	14.0	9.4	13.0	13.8	12.5	16.0	9.3	8.6	10.3	12.6	10.0	14.8	15.0	14.9	18.2	15.7	7.3	14.8	13.0
C30	2.6	8.8	2.6	1.8	1.7	1.8	2.1	1.6	1.6	1.7	1.8	2.0	2.1	2.0	2.0	2.1	2.3	2.3	2.2	2.4	2.2
C31	21.9	27.6	44.2	43.4	42.3	44.7	43.3	40.6	34.8	38.8	38.8	38.1	41.0	41.5	42.7	46.0	40.4	37.5	27.2	40.3	27.6
C32	0.0	0.0	3.0	3.1	2.4	2.5	2.5	2.0	2.4	2.9	2.7	2.2	2.9	2.3	2.2	2.4	1.8	1.9	2.1	2.1	1.7
C33	9.3	6.5	26.7	33.6	26.4	26.1	24.4	21.1	26.0	33.1	29.2	21.8	29.7	22.5	23.3	24.8	15.8	17.9	17.4	17.6	11.9
C34	0.0	0.0	0.0	0.7	0.0	0.0	0.0	0.6	0.0	1.0	1.0	1.2	1.5	0.8	0.0	0.0	0.0	0.0	0.0	0.0	0.0
C35	0.0	0.0	0.0	0.9	0.0	0.0	0.0	0.4	0.0	0.4	0.5	1.1	0.9	0.5	0.0	0.6	1.6	1.0	1.8	0.8	1.4

Table 4: *n*-alkanes of samples 22 to 42. Relative abundances of alkanes shown.

Sample n°	22	23	24	25	26	27	29	30	31	32	33	34	35	36	37	38	39	40	41	42
Upper layer boundary (cm)	-150	-160	-170	-180	-190	-200	-230	-240	-250	-260	-265	-270	-275	-280	-290	-300	-310	-320	-330	-340
C17	0.3	0.0	0.5	0.6	0.6	0.0	0.0	0.0	0.0	0.0	0.6	0.0	0.0	0.0	0.1	0.0	0.0	0.0	0.0	0.0
C18	0.3	0.0	0.0	0.0	0.0	0.0	0.0	0.0	0.0	0.0	0.5	0.0	0.0	0.0	0.1	0.0	0.0	0.0	0.0	0.3
C19	0.4	0.6	0.6	0.0	0.4	0.8	0.0	0.0	0.0	0.0	0.7	0.0	0.0	0.0	0.2	0.3	0.3	0.3	0.4	0.7
C20	0.4	0.8	0.4	0.0	0.5	0.7	0.0	0.0	0.0	0.0	0.6	0.0	0.0	0.0	0.2	0.2	0.0	0.0	0.3	0.4
C21	0.9	1.4	0.9	0.7	1.2	1.4	0.6	1.3	0.8	1.1	1.4	1.1	1.2	1.3	1.1	1.1	1.1	1.1	2.1	1.9
C22	0.8	1.2	0.6	0.5	1.3	1.3	0.4	0.0	0.4	0.6	1.3	0.5	0.7	0.4	0.3	0.3	0.2	0.4	0.6	0.6
C23	3.4	6.1	4.4	4.0	6.5	6.4	3.5	7.3	4.5	5.7	4.1	4.0	2.9	2.0	1.1	2.1	1.3	2.7	3.1	2.6
C24	1.5	2.3	1.2	1.2	2.8	2.5	0.7	1.7	0.8	1.2	2.3	0.8	1.2	0.5	0.5	0.6	0.4	0.7	1.0	0.9
C25	9.4	13.2	8.9	12.3	17.7	18.7	9.4	24.3	13.9	16.1	10.5	8.4	6.6	2.1	1.7	4.0	1.9	4.5	4.2	4.1
C26	1.6	2.5	1.4	1.2	2.9	2.8	0.6	1.8	0.8	1.2	2.7	0.7	1.2	0.4	0.6	0.7	0.5	0.9	1.1	1.1
C27	6.6	9.3	6.1	8.9	11.0	12.2	6.2	15.6	10.4	10.2	8.0	5.9	5.6	2.8	3.2	4.6	3.1	5.5	5.3	4.7
C28	1.5	2.1	1.4	1.2	2.3	2.1	0.8	1.1	0.9	1.2	2.3	1.3	1.6	1.3	0.9	3.4	2.8	1.6	1.5	1.4
C29	8.5	7.9	10.7	9.0	8.8	8.7	13.6	9.5	9.3	11.8	11.3	12.3	10.3	11.9	17.7	14.0	10.9	19.3	13.9	11.7
C30	2.2	2.8	2.4	2.4	2.3	2.3	1.8	0.0	1.5	2.3	2.5	2.6	2.9	2.2	2.6	2.9	2.4	3.1	2.8	2.9
C31	34.1	29.9	36.8	36.7	26.4	24.9	41.4	24.1	31.1	31.9	32.5	40.9	41.7	46.9	46.8	35.8	30.4	47.1	42.6	28.9
C32	2.7	2.3	2.3	2.0	1.9	1.8	2.0	0.0	2.2	1.7	2.2	2.2	2.5	2.5	2.2	2.0	1.9	2.5	2.8	1.8
C33	24.1	17.5	21.3	19.3	13.4	13.4	19.0	13.4	23.3	15.0	16.6	19.4	21.6	25.6	19.3	25.1	41.4	9.5	16.4	33.2
C34	0.0	0.0	0.0	0.0	0.0	0.0	0.0	0.0	0.0	0.0	0.0	0.0	0.0	0.0	1.5	1.5	1.4	1.0	1.9	1.4
C35	1.2	0.0	0.0	0.0	0.0	0.0	0.0	0.0	0.0	0.0	0.0	0.0	0.0	0.0	0.0	1.3	0.0	0.0	0.0	1.3

Table 5: *n*-alkanes of samples 43 to 61. Relative abundances of alkanes shown.

Sample n°	43	44	45	46	47	48	49	50	53	54	56	57	58	60	61
Sample name	Call. vulg.	Sph. Mag.	Sph. cap.	Vacc. uli.	Iso. set.	Vacc. Myr.	Eri. vag.	Sph. rub.	Below. Gr. 2	Below Gr. 2	BGB 03-7	BGB 10-16	BGB 17-22	BGB 31-39	BGB 40-42
C17	0.0	0.0	0.0	0.0	0.0	0.0	0.0	0.0	0.0	0.0	0.0	0.0	0.0	0.0	0.0
C18	0.0	0.0	0.0	0.0	0.0	0.0	0.0	0.0	0.0	0.0	0.0	0.9	0.0	0.0	0.0
C19	0.0	0.0	0.0	0.0	0.0	0.0	0.0	0.0	0.0	0.0	0.0	1.8	0.0	0.0	0.0
C20	0.0	0.0	0.0	0.0	0.0	0.0	0.0	0.0	0.0	0.0	0.0	4.1	0.0	0.0	0.0
C21	0.3	4.0	0.0	0.0	2.2	0.0	0.0	0.0	0.0	0.0	0.0	8.0	0.0	0.0	0.0
C22	0.2	3.0	0.0	0.0	0.0	0.0	0.0	0.0	0.0	0.0	2.7	6.0	0.0	0.0	5.3
C23	0.6	8.0	3.7	4.9	2.4	0.7	0.5	1.8	5.5	3.8	2.6	5.2	6.4	3.7	7.1
C24	0.3	5.1	2.7	5.3	1.7	1.7	0.5	0.0	6.0	3.6	0.0	2.1	3.5	0.0	0.0
C25	1.2	10.1	8.5	18.7	4.9	5.9	1.0	2.9	7.9	5.8	2.6	4.0	11.3	4.4	6.2
C26	0.6	5.9	3.3	7.0	1.8	1.8	0.6	0.0	6.4	3.7	0.0	1.5	2.9	0.0	0.0
C27	4.5	10.2	15.5	38.0	6.6	11.7	2.2	1.9	7.7	7.2	4.2	3.6	6.6	3.8	5.6
C28	1.4	5.4	3.2	5.3	2.0	0.0	0.8	0.0	17.6	6.4	0.0	1.8	0.0	0.0	0.0
C29	14.3	14.2	11.7	7.9	9.5	33.2	10.1	14.2	20.8	9.5	9.5	6.5	19.6	22.2	11.2
C30	2.2	4.4	0.0	0.0	0.0	12.4	1.8	0.0	11.9	0.0	0.0	1.4	0.0	0.0	0.0
C31	45.9	19.9	29.0	12.9	39.9	29.7	53.9	49.5	16.2	7.5	28.3	11.6	19.2	27.0	21.4
C32	2.7	0.0	0.0	0.0	0.0	0.0	2.2	2.4	0.0	17.5	3.6	1.7	11.0	3.0	6.2
C33	25.1	9.7	22.5	0.0	29.0	2.9	26.4	27.3	0.0	35.0	33.9	22.9	12.4	14.6	18.3
C34	0.0	0.0	0.0	0.0	0.0	0.0	0.0	0.0	0.0	0.0	12.5	9.2	7.0	21.2	18.7
C35	0.7	0.0	0.0	0.0	0.0	0.0	0.0	0.0	0.0	0.0	0.0	7.9	0.0	0.0	0.0

Table 6: *n*-alcohols of samples 1 to 21. Relative abundances of alcohols shown.

Sample n°	1	2	3	4	5	6	7	8	9	10	11	12	13	14	15	16	17	18	19	20	21
Upper layer boundary (cm)	0	-6	-11	-16	-23	-28	-33	-38	-43	-48	-53	-58	-63	-68	-73	-78	-100	-110	-120	-130	-140
C8	3.4	1.9	0.5	0.4	0.8	0.0	0.0	0.0	0.0	0.0	0.0	0.0	0.0	0.0	0.0	0.0	0.0	0.0	0.0	0.0	0.0
C9	0.0	0.0	0.0	0.0	0.0	0.0	0.0	0.0	0.0	0.0	0.0	0.0	0.0	0.0	0.0	0.0	0.0	0.0	0.0	0.0	0.0
C10	4.8	4.2	1.1	1.5	1.6	1.7	1.9	2.1	2.9	0.0	0.0	0.0	0.0	0.0	0.0	0.0	0.0	0.0	0.0	0.0	0.0
C11	0.0	0.0	0.0	0.0	0.0	0.0	0.0	0.0	0.0	0.0	0.0	0.0	0.0	0.0	0.0	0.0	0.0	0.0	0.0	0.0	0.0
C12	0.0	0.0	0.0	1.3	1.5	0.0	1.4	0.0	0.0	1.4	1.5	1.3	1.1	1.2	0.0	1.0	0.0	0.0	0.0	0.0	0.0
C13	0.0	0.0	0.0	0.0	0.0	0.0	0.0	0.0	0.0	0.0	0.0	0.0	0.0	0.0	0.0	0.0	0.0	0.0	0.0	0.0	0.0
C14	4.0	3.1	0.7	0.7	0.8	0.0	0.0	0.0	0.0	0.0	0.0	0.0	0.0	0.0	0.0	0.0	0.0	0.0	0.0	0.0	0.0
C15	0.0	0.0	0.0	0.8	0.9	0.0	1.1	1.5	0.0	0.0	0.0	0.0	0.0	0.0	0.0	2.0	0.0	0.0	0.0	0.0	0.0
C16	0.0	0.0	0.0	1.1	2.1	2.9	4.1	3.9	2.4	2.6	4.1	4.3	3.4	3.0	2.8	4.8	5.7	8.9	9.7	8.4	8.8
C17	0.0	0.0	0.0	0.0	0.0	0.0	0.0	0.0	0.0	0.0	0.0	0.0	0.0	0.0	0.0	0.0	0.0	0.0	0.0	0.0	0.0
C18	36.6	2.9	0.9	0.9	1.7	2.0	2.3	2.2	1.9	1.7	2.1	2.4	1.8	1.9	1.9	2.5	0.0	5.4	6.8	6.8	8.1
C19	0.0	0.0	0.0	0.0	0.0	0.0	0.0	0.0	0.0	0.0	0.0	0.0	0.0	0.0	0.0	0.0	0.0	0.0	0.0	0.0	0.0
C20	0.0	0.0	1.7	2.2	1.7	2.8	2.8	2.6	2.0	2.4	2.4	2.8	2.6	4.0	1.9	3.4	0.0	3.4	0.0	3.7	5.5
C21	0.0	0.0	0.0	0.0	0.0	0.0	0.0	0.0	0.0	0.0	0.0	0.0	0.0	0.0	0.0	0.0	0.0	0.0	0.0	0.0	0.0
C22	0.0	5.8	6.6	12.9	8.1	9.9	7.7	8.7	9.7	12.7	10.3	10.2	12.0	13.7	5.9	11.6	7.4	9.9	10.8	8.8	8.3
C23	4.8	0.0	0.0	1.5	1.2	1.3	1.5	1.3	0.0	1.4	1.3	0.0	1.3	1.9	0.0	1.6	0.0	0.0	0.0	0.0	0.0
C24	0.0	10.8	9.9	19.8	12.6	14.1	14.7	17.1	18.9	15.4	14.6	15.4	15.9	19.8	9.8	19.1	16.3	19.8	21.7	22.5	19.5
C25	11.1	3.1	0.0	1.7	1.6	1.2	1.8	1.5	2.5	1.2	1.2	1.4	1.3	2.4	0.0	1.7	0.0	7.8	0.0	3.7	0.0
C26	0.0	9.6	8.2	13.3	11.2	10.3	11.9	14.1	16.3	8.9	10.7	11.2	10.0	14.1	8.0	14.6	17.6	17.4	20.2	22.1	21.6
C27	11.9	0.0	0.0	0.8	0.0	0.0	0.0	0.0	1.2	0.8	0.0	0.0	0.0	1.1	0.0	1.3	0.0	0.0	0.0	0.0	0.0
C28	0.0	10.0	9.3	20.6	11.1	10.7	8.1	10.4	12.8	10.7	11.6	11.3	11.1	15.2	6.8	17.1	16.4	11.2	10.6	10.3	9.1
C29	7.1	0.0	2.2	0.0	4.5	4.1	0.0	0.0	0.0	0.0	0.0	0.0	0.0	0.0	0.0	0.0	0.0	0.0	0.0	0.0	0.0
C30	0.0	34.9	22.1	8.5	6.6	11.9	20.5	20.7	25.7	18.1	10.7	11.5	11.7	13.9	51.0	10.7	36.5	16.1	20.3	13.6	19.0
C31	16.3	0.0	0.0	0.0	0.0	0.0	0.0	0.0	0.0	0.0	0.0	0.0	0.0	0.0	0.0	0.0	0.0	0.0	0.0	0.0	0.0
C32	0.0	0.0	2.7	12.0	4.1	0.0	5.3	0.0	3.6	2.6	3.2	6.2	3.3	7.7	0.0	8.7	0.0	0.0	0.0	0.0	0.0
C33	0.0	0.0	0.0	0.0	0.0	0.0	0.0	0.0	0.0	0.0	0.0	0.0	0.0	0.0	0.0	0.0	0.0	0.0	0.0	0.0	0.0
C34	0.0	13.6	34.0	0.0	27.9	27.1	14.9	14.0	0.0	20.2	26.2	21.9	24.3	0.0	12.0	0.0	0.0	0.0	0.0	0.0	0.0
C35	0.0	0.0	0.0	0.0	0.0	0.0	0.0	0.0	0.0	0.0	0.0	0.0	0.0	0.0	0.0	0.0	0.0	0.0	0.0	0.0	0.0

Table 7: *n*-alcohols of samples 22 to 42. Relative abundances of alcohols shown.

Sample n°	22	23	24	25	26	27	29	30	31	32	33	34	35	36	37	38	39	40	41	42
Upper layer boundary (cm)	-150	-160	-170	-180	-190	-200	-230	-240	-250	-260	-265	-270	-275	-280	-290	-300	-310	-320	-330	-340
C8	0.0	0.0	0.0	0.0	0.0	0.0	0.0	0.0	0.0	0.0	0.0	0.0	0.0	0.0	0.0	0.0	0.0	0.0	0.0	0.0
C9	0.0	0.0	0.0	0.0	0.0	0.0	0.0	0.0	0.0	0.0	0.0	0.0	0.0	0.0	0.0	0.0	0.0	0.0	0.0	0.0
C10	0.0	0.0	0.0	0.0	0.0	0.0	0.0	0.0	0.0	0.0	0.0	0.0	0.0	0.0	0.0	0.0	0.0	0.0	0.0	0.0
C11	0.0	0.0	0.0	0.0	0.0	0.0	0.0	0.0	0.0	0.0	0.0	0.0	0.0	0.0	0.0	0.0	0.0	0.0	0.0	0.0
C12	0.0	4.5	0.0	0.0	0.0	0.0	0.0	0.0	0.0	0.0	0.0	0.0	0.0	0.0	0.0	0.9	0.4	0.7	1.0	0.0
C13	0.0	0.0	0.0	0.0	0.0	0.0	0.0	0.0	0.0	0.0	0.0	0.0	0.0	0.0	0.0	0.0	0.0	0.0	0.0	0.0
C14	0.0	0.0	0.0	0.0	0.0	0.0	0.0	0.0	0.0	0.0	0.0	0.0	0.9	0.5	0.0	0.0	0.3	0.2	0.4	0.0
C15	0.0	0.0	0.0	0.0	0.0	0.0	0.0	0.0	0.0	0.0	0.0	0.0	0.0	0.0	0.0	0.0	0.0	0.0	0.0	0.0
C16	6.6	11.0	12.4	11.8	0.0	9.3	0.0	6.5	0.0	4.8	5.4	3.6	5.1	2.7	2.9	2.8	1.7	1.7	2.3	2.3
C17	0.0	0.0	0.0	0.0	0.0	0.0	0.0	0.0	0.0	0.0	0.0	0.0	0.0	0.0	0.0	0.0	0.0	0.0	0.0	0.0
C18	5.8	8.0	8.6	8.3	0.0	7.1	0.0	0.0	0.0	3.8	5.2	2.9	4.3	2.5	2.2	2.2	1.3	1.3	1.8	2.3
C19	0.0	0.0	0.0	0.0	0.0	0.0	0.0	0.0	0.0	0.0	0.0	0.0	0.0	0.0	0.0	0.0	0.0	0.0	0.0	0.0
C20	5.3	5.2	0.0	7.3	0.0	0.0	0.0	0.0	0.0	4.1	3.9	4.7	4.9	3.9	3.9	4.7	4.5	4.3	4.6	7.2
C21	0.0	0.0	0.0	0.0	0.0	0.0	0.0	0.0	0.0	0.0	0.0	2.0	0.0	0.7	1.0	1.0	0.8	0.8	0.7	1.3
C22	13.4	10.7	14.9	11.4	11.2	10.5	11.9	10.5	8.5	12.9	14.1	16.4	13.5	14.6	14.9	14.9	18.6	12.6	18.3	14.9
C23	0.0	0.0	0.0	0.0	0.0	0.0	0.0	0.0	0.0	0.0	0.0	2.1	2.7	3.0	1.8	2.4	2.3	1.7	2.0	1.8
C24	23.2	20.2	23.6	27.9	26.2	23.3	22.2	25.3	19.9	24.9	18.9	24.0	24.6	24.7	22.1	25.6	22.4	21.2	22.8	20.6
C25	0.0	0.0	0.0	0.0	0.0	0.0	0.0	0.0	0.0	0.0	0.0	0.0	0.0	3.3	2.9	4.3	2.8	3.0	2.1	2.6
C26	19.7	18.1	20.1	24.2	25.6	22.1	17.2	22.4	18.2	20.7	14.7	18.6	20.8	16.4	16.5	22.9	15.6	20.3	15.7	15.5
C27	0.0	0.0	0.0	0.0	0.0	0.0	0.0	0.0	0.0	0.0	0.0	2.5	3.0	2.6	3.4	0.0	2.1	2.7	1.8	2.2
C28	13.1	7.9	10.7	9.2	0.0	6.3	9.9	9.7	10.4	14.3	8.5	9.8	9.5	14.3	22.5	3.2	18.1	23.3	21.1	23.4
C29	0.0	0.0	0.0	0.0	0.0	0.0	0.0	0.0	0.0	0.0	0.0	0.0	0.0	0.0	0.0	0.0	0.0	0.0	0.0	0.9
C30	12.9	14.3	9.8	0.0	37.1	21.4	38.7	25.6	43.0	14.5	29.2	13.6	10.9	6.9	0.0	15.2	5.8	0.0	0.0	5.0
C31	0.0	0.0	0.0	0.0	0.0	0.0	0.0	0.0	0.0	0.0	0.0	0.0	0.0	0.0	0.0	0.0	0.0	0.0	0.0	0.0
C32	0.0	0.0	0.0	0.0	0.0	0.0	0.0	0.0	0.0	0.0	0.0	0.0	0.0	4.0	5.9	0.0	3.4	6.2	5.4	0.0
C33	0.0	0.0	0.0	0.0	0.0	0.0	0.0	0.0	0.0	0.0	0.0	0.0	0.0	0.0	0.0	0.0	0.0	0.0	0.0	0.0
C34	0.0	0.0	0.0	0.0	0.0	0.0	0.0	0.0	0.0	0.0	0.0	0.0	0.0	0.0	0.0	0.0	0.0	0.0	0.0	0.0
C35	0.0	0.0	0.0	0.0	0.0	0.0	0.0	0.0	0.0	0.0	0.0	0.0	0.0	0.0	0.0	0.0	0.0	0.0	0.0	0.0

Table 8: *n*-alcohols of samples 43 to 61. Relative abundances of alcohols shown.

Sample n°	43	44	45	46	47	48	49	50	53	54	56	57	58	60	61
Upper layer boundary (cm)	Call. vulg.	Sph. Mag.	Sph. cap.	Vacc. uli.	Iso. set.	Vacc. Myr.	Eri. vag.	Sph. rub.	w. Gr. 2	w Gr. 2	BGB 03-7	10-16	17-22	31-39	40-42
C8	0.0	0.0	0.0	0.0	0.0	0.0	0.0	0.0	0.0	0.0	0.0	0.0	0.0	0.0	0.0
C9	0.0	0.0	0.0	0.0	0.0	0.0	0.0	0.0	0.0	0.0	0.0	0.0	0.0	0.0	0.0
C10	0.0	0.0	0.0	0.0	0.0	0.0	0.0	0.0	0.0	0.0	0.0	0.0	0.0	0.0	0.0
C11	0.0	0.0	0.0	0.0	0.0	0.0	0.0	0.0	0.0	0.0	0.0	0.0	0.0	0.0	0.0
C12	0.0	0.0	0.0	0.0	0.0	0.0	0.0	0.0	0.0	0.0	0.0	0.0	0.0	0.0	0.0
C13	0.0	0.0	0.0	0.0	0.0	0.0	0.0	0.0	0.0	0.0	0.0	0.0	0.0	0.0	0.0
C14	0.0	0.0	0.0	0.0	0.0	0.0	0.0	0.0	0.0	0.0	0.0	0.0	0.0	0.0	0.0
C15	0.0	0.0	0.0	0.5	0.0	0.8	0.0	0.0	3.2	2.5	2.4	3.7	0.0	0.0	0.0
C16	0.4	1.3	0.0	1.7	1.1	1.0	0.0	0.0	3.5	2.6	2.5	5.6	2.1	2.9	2.8
C17	0.0	0.0	0.0	0.0	0.0	0.0	0.0	0.0	0.0	0.0	0.0	0.0	0.0	0.0	0.0
C18	1.0	9.0	12.1	2.6	3.0	2.5	11.3	11.8	5.3	4.1	2.2	4.5	2.6	2.9	6.2
C19	0.0	0.0	0.0	0.0	0.0	0.0	0.0	0.0	0.0	0.0	0.0	0.0	0.0	0.0	0.0
C20	0.7	1.1	0.0	2.7	1.4	2.4	0.0	0.0	5.9	9.1	5.0	8.4	13.1	4.7	13.3
C21	1.0	1.6	0.0	3.4	1.7	3.6	0.0	2.6	4.0	2.8	0.0	0.0	0.0	0.0	0.0
C22	6.2	5.1	14.8	4.9	3.3	18.0	7.1	11.4	21.1	14.2	14.3	21.1	6.5	19.0	13.1
C23	1.2	1.3	1.9	1.7	0.0	2.8	0.0	2.4	2.4	1.6	0.0	0.0	0.0	0.0	0.0
C24	23.4	13.3	16.5	20.2	11.6	35.2	17.2	31.4	18.6	14.8	10.6	9.7	3.8	12.1	8.5
C25	1.7	1.9	2.7	4.4	0.0	2.7	0.0	3.3	0.0	0.0	0.0	0.0	0.0	0.0	0.0
C26	18.0	10.8	16.6	26.8	20.4	13.8	9.1	20.8	10.3	16.6	7.5	5.1	10.3	11.1	6.3
C27	1.4	1.4	4.5	3.6	4.0	3.4	0.0	0.0	0.0	2.9	2.6	0.0	0.0	4.4	0.0
C28	28.0	7.2	12.0	27.4	42.6	14.0	8.2	16.3	12.1	22.9	31.0	29.8	54.7	37.4	0.0
C29	8.1	0.0	0.0	0.0	0.0	0.0	0.0	0.0	0.0	0.0	0.0	0.0	7.1	0.0	0.0
C30	5.6	46.0	10.7	0.0	0.0	0.0	0.0	0.0	13.6	5.9	3.6	4.2	0.0	0.0	0.0
C31	1.3	0.0	0.0	0.0	0.0	0.0	0.0	0.0	0.0	0.0	0.0	0.0	0.0	0.0	0.0
C32	2.1	0.0	8.2	0.0	6.8	0.0	47.1	0.0	0.0	0.0	0.0	0.0	0.0	0.0	28.8
C33	0.0	0.0	0.0	0.0	0.0	0.0	0.0	0.0	0.0	0.0	0.0	0.0	0.0	0.0	0.0
C34	0.0	0.0	0.0	0.0	4.2	0.0	0.0	0.0	0.0	0.0	18.2	7.8	0.0	5.5	20.9
C35	0.0	0.0	0.0	0.0	0.0	0.0	0.0	0.0	0.0	0.0	0.0	0.0	0.0	0.0	0.0

Table 9: *n*-fatty acids of samples 1 to 21. Relative abundances of fatty acids shown.

Sample n°	1	2	3	4	5	6	7	8	9	10	11	12	13	14	15	16	17	18	19	20	21
Upper layer boundary (cm)	0	-6	-11	-16	-23	-28	-33	-38	-43	-48	-53	-58	-63	-68	-73	-78	-100	-110	-120	-130	-140
C10	0.5	0.2	0.0	0.6	0.4	0.4	0.3	0.0	0.0	0.0	0.0	0.0	0.0	0.0	0.0	0.4	0.4	0.0	0.0	0.0	0.0
C11	0.9	0.3	0.9	1.0	0.7	0.5	0.6	1.7	3.5	0.2	0.3	0.6	0.3	0.0	0.4	0.7	0.7	0.6	2.9	0.6	0.7
C12	4.1	1.7	3.1	1.9	3.0	2.6	3.1	3.2	3.1	1.0	1.3	2.5	1.7	2.6	2.0	1.9	1.9	3.2	2.7	2.9	3.5
C13	0.4	0.1	0.2	0.0	0.0	0.0	0.2	0.0	0.0	0.0	0.0	0.0	0.0	0.0	0.0	0.0	0.0	0.0	0.0	0.0	0.0
C14	2.4	1.2	4.0	3.1	2.9	3.0	3.4	5.0	5.0	2.4	2.7	4.2	4.5	4.4	3.4	3.4	3.4	4.2	3.8	2.2	2.1
C15	1.7	0.6	0.5	0.0	0.6	0.6	0.7	1.0	1.4	0.5	0.5	0.8	0.7	0.0	0.6	0.7	0.7	1.2	1.1	1.1	1.3
C16:1	0.7	1.5	0.8	0.3	0.5	0.2	0.5	0.8	1.3	0.3	0.0	0.9	0.6	0.0	0.0	0.0	0.0	1.2	0.9	0.3	1.3
C16:0	24.9	11.3	10.4	9.6	9.8	11.5	10.6	14.4	14.9	8.0	8.7	15.4	15.2	22.9	13.9	13.4	13.4	17.5	14.0	19.9	17.6
C17	1.0	0.4	0.2	0.2	0.4	0.5	0.5	0.7	0.7	0.4	0.4	0.7	0.6	0.0	0.0	0.0	0.0	0.8	0.8	1.0	0.9
C18:2	2.7	14.8	2.3	0.5	1.4	0.0	0.0	0.7	0.0	0.6	0.4	1.6	1.6	0.0	0.7	0.6	0.6	1.0	0.0	0.6	0.8
C18:1a	15.4	40.2	21.6	5.7	26.0	1.4	2.4	9.5	9.5	18.3	13.3	2.5	2.4	2.2	14.8	14.9	14.9	8.8	8.6	7.8	0.0
C18:1b	2.9	4.0	1.7	1.3	2.2	0.0	0.0	1.5	1.3	1.0	0.8	0.0	0.0	0.0	1.7	1.5	1.5	1.5	1.1	1.3	1.1
C18:0	7.2	3.8	3.3	4.5	4.0	6.2	5.6	6.7	7.8	3.4	5.4	6.5	7.0	10.2	6.3	6.1	6.1	9.7	8.3	12.3	9.5
C19	8.0	3.6	2.9	0.0	1.4	2.7	0.0	1.0	0.0	0.6	1.6	3.9	1.9	0.0	0.0	2.1	2.1	0.0	0.0	2.2	1.5
C20	2.0	1.6	4.4	4.3	2.8	4.8	4.0	3.6	2.7	3.5	3.1	3.5	3.1	4.6	4.4	4.1	4.1	2.4	1.6	2.0	1.8
C21	0.0	0.4	2.2	4.8	3.1	2.7	2.1	2.3	2.5	1.9	1.9	2.5	3.6	2.6	1.8	1.7	1.7	1.4	0.0	0.9	0.8
C22	3.6	2.8	9.5	12.4	6.4	11.2	8.8	7.1	7.5	11.9	9.0	8.1	10.0	9.8	8.0	7.6	7.6	5.3	4.0	5.2	4.1
C23	2.0	0.6	1.5	2.1	1.6	2.4	2.7	1.6	1.8	2.3	2.0	2.0	1.9	2.4	1.9	1.9	1.9	1.7	1.5	1.9	1.5
C24	6.7	3.4	8.4	14.3	12.1	17.4	21.1	15.2	16.4	17.9	15.7	14.3	13.8	14.9	13.7	14.0	14.0	13.7	12.0	12.1	11.5
C24:1	4.8	2.3	1.9	2.7	3.4	4.2	3.2	3.6	1.4	1.0	1.5	4.5	5.5	0.0	4.2	4.4	4.4	9.2	12.7	9.3	9.3
C25	0.8	0.5	1.8	2.1	1.6	2.0	2.6	1.6	2.1	2.0	2.2	1.8	1.7	2.0	1.7	1.7	1.7	1.6	1.1	1.3	1.3
C26	3.3	1.2	4.7	8.2	7.2	9.0	13.8	8.8	9.7	8.3	10.2	7.9	7.1	7.9	8.0	8.1	8.1	8.0	6.4	6.8	6.7
C27	0.0	0.4	1.1	1.8	1.0	1.1	1.3	0.6	0.0	1.2	1.5	0.0	1.4	0.0	1.1	1.1	1.1	0.0	0.0	0.0	0.0
C28	0.9	0.6	3.7	7.2	2.4	4.0	4.6	2.8	2.9	4.4	4.8	2.7	3.1	3.5	3.5	3.4	3.4	2.2	1.3	1.9	1.4
C29	0.0	0.3	0.9	1.1	0.4	0.6	0.7	0.4	0.9	1.0	1.3	0.0	0.6	0.0	0.0	0.5	0.5	0.0	0.0	0.0	0.0
C30	0.5	0.7	3.1	4.2	1.6	3.1	2.3	1.7	1.6	3.1	3.5	2.5	2.3	3.1	2.6	2.3	2.3	1.5	0.0	1.1	0.0
C31	2.7	1.3	2.7	2.0	1.8	3.7	2.1	2.2	1.9	1.7	3.4	3.3	6.5	3.4	2.4	1.6	1.6	3.4	2.1	3.7	2.9
C32	0.0	0.0	2.1	4.2	1.5	2.9	2.8	2.3	0.0	3.2	3.6	2.8	2.8	3.5	2.9	2.0	2.0	0.0	13.0	1.7	18.5
C33	0.0	0.0	0.0	0.0	0.0	0.0	0.0	0.0	0.0	0.0	0.0	4.5	0.0	0.0	0.0	0.0	0.0	0.0	0.0	0.0	0.0
C34	0.0	0.0	0.0	0.0	0.0	1.2	0.0	0.0	0.0	0.0	0.9	0.0	0.0	0.0	0.0	0.0	0.0	0.0	0.0	0.0	0.0

Table 10: n-fatty acids of samples 22 to 42. Relative abundances of fatty acids shown.

Sample n°	22	23	24	25	26	27	29	30	31	32	33	34	35	36	37	38	39	40	41	42
Upper layer boundary (cm)	-150	-160	-170	-180	-190	-200	-230	-240	-250	-260	-265	-270	-275	-280	-290	-300	-310	-320	-330	-340
C10	0.3	0.0	0.0	0.0	0.4	0.4	0.0	0.0	0.0	0.0	0.0	0.0	0.0	0.0	0.0	0.0	0.0	0.0	0.0	0.0
C11	0.4	1.6	0.7	0.0	2.3	2.2	0.0	1.8	0.0	1.0	0.0	0.0	0.0	0.5	0.0	0.9	0.0	0.4	0.3	0.3
C12	2.0	2.9	1.8	2.5	3.1	2.5	1.8	1.8	1.9	2.0	1.6	2.4	3.0	1.3	1.4	1.0	1.3	1.7	1.5	1.4
C13	0.2	0.0	0.0	0.0	0.2	0.0	0.0	0.0	0.0	0.0	0.0	0.0	0.0	0.0	0.0	0.0	0.0	0.0	0.0	0.0
C14	4.4	1.5	1.2	2.6	3.8	3.4	5.5	2.8	4.5	5.5	3.3	4.3	2.8	1.6	3.1	1.7	1.8	3.4	3.6	3.7
C15	1.1	1.4	1.1	0.0	1.1	1.1	2.4	1.0	1.0	2.3	0.9	0.0	0.8	0.7	0.0	0.5	0.0	0.6	1.0	1.2
C16:1	1.5	0.6	0.6	0.0	0.3	1.0	6.5	1.1	1.2	6.0	0.6	0.0	0.0	0.6	0.0	0.4	0.0	0.5	1.9	2.8
C16:0	17.5	16.7	18.8	13.3	15.1	13.5	21.6	14.0	16.4	21.5	15.1	15.1	12.1	12.7	13.1	8.9	6.8	12.7	13.0	13.8
C17	0.7	0.8	0.7	0.0	0.7	0.5	0.8	0.6	0.0	1.0	0.0	0.0	3.5	0.4	0.0	0.0	0.0	0.4	1.3	1.1
C18:2	0.5	0.0	0.5	0.0	0.5	0.6	0.0	0.0	6.1	0.8	0.0	0.0	0.0	0.5	7.9	0.0	0.6	0.4	0.5	0.7
C18:1a	5.5	5.8	5.0	6.6	5.5	6.7	8.5	4.2	6.1	8.2	3.8	5.1	0.0	7.6	0.0	4.7	18.8	3.9	3.4	3.9
C18:1b	1.1	0.9	0.8	0.0	0.9	1.1	0.9	0.7	0.0	0.9	0.0	0.0	4.5	0.6	0.0	0.0	1.1	0.9	0.7	0.9
C18:0	11.4	10.5	15.5	10.7	10.7	10.1	11.8	9.7	9.8	11.4	11.2	0.0	8.5	11.1	8.0	6.5	4.8	7.1	9.1	8.0
C19	1.4	1.3	1.0	2.5	1.9	1.8	0.0	1.0	0.0	0.0	0.0	10.2	0.0	1.4	0.0	2.9	2.4	1.6	1.9	2.1
C20	1.9	1.8	2.2	0.0	2.0	1.5	1.8	1.6	2.2	1.5	1.8	3.0	2.4	2.9	2.8	2.5	2.0	4.4	3.0	8.4
C21	0.8	0.0	0.8	0.0	0.6	0.6	0.0	0.0	0.0	0.0	0.0	0.0	0.0	1.2	1.6	1.6	1.4	1.6	1.5	1.5
C22	4.2	4.8	5.0	6.6	4.8	4.5	3.8	4.9	4.4	3.0	6.7	6.8	6.9	8.7	9.8	10.4	7.0	10.4	10.4	9.8
C23	1.8	1.7	1.4	2.7	1.7	1.7	1.3	2.0	1.8	1.3	2.0	2.2	2.1	2.3	2.1	2.2	2.2	2.2	2.1	2.4
C24	8.7	11.6	10.2	18.3	11.3	11.3	8.2	16.8	11.5	7.2	18.0	17.3	16.6	14.1	14.5	18.4	18.6	19.2	19.3	17.4
C24:1	6.2	6.3	5.1	9.3	5.8	10.5	6.5	8.2	11.0	8.3	6.4	7.9	7.6	9.0	2.0	2.4	4.8	2.4	1.2	0.8
C25	0.9	1.2	1.0	0.0	1.3	1.1	0.0	1.8	0.0	0.0	1.9	0.0	1.8	1.4	1.8	2.2	2.3	2.0	2.0	1.6
C26	4.7	6.5	5.6	11.9	6.9	7.2	4.6	10.6	6.8	3.4	10.1	10.3	10.3	9.2	8.3	10.5	13.0	10.2	9.7	9.2
C27	0.6	0.0	0.0	0.0	0.0	0.0	0.0	0.0	0.0	0.0	0.0	0.0	0.0	0.9	1.8	1.4	1.3	1.6	1.7	1.0
C28	1.4	1.9	1.6	3.4	1.9	2.5	1.3	2.1	1.6	1.6	2.2	2.5	2.7	3.9	4.7	4.2	3.7	4.9	4.4	3.3
C29	0.0	0.0	0.0	0.0	0.0	0.0	0.0	0.0	0.0	0.0	0.0	0.0	0.0	0.0	0.0	0.7	0.5	0.6	0.6	0.6
C30	0.6	0.0	0.6	0.0	1.1	0.0	0.0	0.0	0.0	0.0	0.0	0.0	0.0	1.3	3.3	2.8	2.2	2.7	2.5	1.6
C31	2.4	2.3	2.0	0.0	2.3	2.2	2.1	1.6	2.7	1.6	2.0	0.0	2.4	3.0	0.0	1.7	1.8	2.0	1.7	1.3
C32	16.9	18.0	16.9	9.6	12.3	10.4	10.6	11.7	11.0	11.6	12.5	12.7	11.8	1.4	13.8	11.7	1.8	2.1	1.9	1.1
C33	0.0	0.0	0.0	0.0	0.0	0.0	0.0	0.0	0.0	0.0	0.0	0.0	0.0	0.0	0.0	0.0	0.0	0.0	0.0	0.0
C34	1.0	0.0	0.0	0.0	1.5	1.4	0.0	0.0	0.0	0.0	0.0	0.0	0.0	1.5	0.0	0.0	0.0	0.0	0.0	0.0

Table 11: n-fatty acids of samples 43 to 61. Relative abundances of fatty acids shown.

Sample n°	43	44	45	46	47	48	49	50	53	54	56	57	58	60	61
Upper layer boundary (cm)	Call. vulg.	Sph. Mag.	Sph. cap.	Vacc. uli.	Iso. set.	Vacc. Myr.	Eri. vag.	Sph. rub.	Below. Gr. 2	Below Gr. 2	BGB 03-7	BGB 10-16	BGB 17-22	BGB 31-39	BGB 40-42
C10	0.0	1.6	0.7	0.9	0.6	0.0	1.0	0.9	0.0	0.0	0.3	0.2	0.3	0.0	0.0
C11	0.8	1.9	1.2	0.6	0.7	0.9	0.9	1.2	0.0	0.0	0.5	0.3	0.3	0.2	0.0
C12	3.9	8.0	5.6	3.9	4.3	5.6	4.9	5.9	2.3	2.4	2.7	1.4	0.9	1.1	1.0
C13	0.2	0.9	0.6	0.2	0.3	0.0	0.5	0.6	0.0	0.0	0.2	0.0	0.0	0.0	0.0
C14	7.1	4.5	2.2	3.5	4.2	6.5	4.5	1.7	4.6	3.8	4.2	4.3	6.0	4.0	2.9
C15	0.8	2.2	1.8	0.6	1.0	0.9	1.1	1.0	1.1	0.9	0.6	0.5	0.5	0.4	0.4
C16:1	1.1	1.2	0.6	0.8	0.3	0.0	0.0	0.0	0.0	0.0	0.4	0.0	0.0	0.0	0.0
C16:0	29.8	35.8	38.2	33.2	37.9	36.8	34.9	27.0	20.1	19.9	14.2	13.0	14.3	11.0	9.7
C17	0.6	1.2	1.2	0.8	0.7	0.0	0.7	1.1	0.0	0.7	0.3	0.3	0.2	0.0	0.0
C18:2	0.0	0.8	0.3	2.6	0.7	0.0	2.4	0.9	4.9	4.2	1.0	0.6	0.7	0.0	0.6
C18:1a	1.3	2.9	0.7	5.6	3.5	2.2	9.8	5.1	9.9	10.7	8.1	8.9	3.6	2.8	2.2
C18:1b	0.3	0.8	0.2	0.6	0.7	0.0	1.0	0.9	1.3	1.2	1.7	0.7	0.7	0.4	0.5
C18:0	7.2	8.3	7.9	7.6	11.5	9.6	9.5	7.3	13.3	11.9	9.6	10.0	11.4	8.0	7.8
C19	5.1	0.0	12.4	3.3	5.8	5.0	10.1	10.3	0.0	0.0	0.0	0.0	0.0	0.0	0.0
C20	3.9	3.6	3.1	9.9	2.9	5.6	2.5	2.3	4.1	4.4	4.2	4.1	4.9	2.3	7.2
C21	0.4	0.6	3.3	1.5	0.7	1.8	0.7	0.9	2.2	2.7	8.8	6.3	4.8	2.8	3.4
C22	1.0	5.9	5.7	5.1	4.8	4.7	2.5	5.9	4.5	5.9	8.3	10.6	5.1	7.9	10.5
C23	6.5	1.6	2.0	1.6	1.3	1.2	1.9	2.0	1.3	1.2	2.7	3.5	1.6	2.7	3.8
C24	7.9	9.6	6.6	5.2	5.9	4.2	2.8	12.3	3.1	4.5	0.2	7.6	6.1	11.5	16.4
C24:1	0.0	0.0	0.0	0.0	0.0	0.0	0.6	0.2	7.1	5.1	4.9	4.0	8.8	8.5	3.4
C25	1.1	1.2	1.0	0.9	0.9	0.0	0.8	1.3	1.0	1.1	1.8	2.4	2.0	2.6	3.1
C26	6.2	4.3	2.4	6.1	2.9	2.8	1.4	5.4	2.1	4.3	6.1	4.7	7.9	9.7	10.2
C27	0.8	0.0	0.9	0.5	0.0	0.0	0.0	0.9	1.0	1.0	1.6	1.3	1.2	1.2	1.4
C28	5.8	1.4	0.8	3.6	2.2	2.5	0.7	1.9	2.6	2.2	6.2	4.0	5.1	5.9	3.9
C29	0.4	0.0	0.0	0.0	0.0	0.0	0.0	0.2	2.0	1.2	0.6	0.7	0.6	0.6	0.0
C30	2.7	0.0	0.3	0.2	0.8	3.9	1.1	1.1	5.7	3.8	3.4	4.4	9.1	6.7	1.8
C31	3.6	1.6	0.4	1.0	5.3	4.7	3.6	1.0	3.2	4.9	4.6	4.2	2.7	2.5	2.0
C32	1.5	0.0	0.0	0.0	0.0	1.0	0.0	0.8	2.6	2.1	1.7	1.0	1.6	7.3	7.9
C33	0.0	0.0	0.0	0.0	0.0	0.0	0.0	0.0	0.0	0.0	0.0	0.0	0.0	0.0	0.0
C34	0.0	0.0	0.0	0.0	0.0	0.0	0.0	0.0	0.0	0.0	1.2	1.4	0.0	0.0	0.0

Personal declaration

I hereby declare that the submitted thesis is the result of my own, independent work. All external sources are explicitly acknowledged in the thesis.

Zurich, 30th of June Silvana Bernasconi